MIAMI UNIVERSITY

The Graduate School

Certificate for Approving the Dissertation

We hereby approve the Dissertation

of

Mart Patrick Hensley

Candidate for the Degree:

Doctor of Philosophy

_____

Director
Dr. Michael W. Crowder

_____

Reader
Dr. Carole Dabney-Smith

_____

Reader
Dr. Christopher A. Makaroff

_____

Reader
Dr. David L. Tierney

_____

Graduate School Representative
Dr. Gary R. Janssen

ABSTRACT

ZINC HOMEOSTASIS IN *E.COLI*

by M. Patrick Hensley

The homeostasis of transition metal ions is critical to the survival of all organisms. Zinc (Zn(II)) is one of the most important transition metals found in biological systems; however, the homeostasis of this metal is poorly understood. Previous studies have shown that intracellular Zn(II) levels in *E. coli* are in the low millimolar range, yet there is less than one "free" (unbound) Zn(II) ion per cell. There must exist in the *E. coli* cell a mechanism for the delivery and insertion of Zn(II) into proteins. The cytoplasmic transport of other transitions metals, such as copper, iron, nickel, manganese, and arsenic, is accomplished by a group of proteins called metallochaperones. No such metallochaperone has been identified for Zn(II). Since none of the available models for intracellular Zn(II) transport are able to explain adequately Zn(II) homeostasis in *E. coli*, we hypothesized a new model. This model proposes that Zn(II) is delivered to Zn(II) metalloproteins as the proteins are translated and exiting the ribosome.

In the co-translational model for Zn(II) homeostasis, the first datum that must be accounted for is the constant presence of 0.2 mM Zn(II) in *E. coli*. In Chapter 2 it is shown that the ribosome binds significant amounts of Zn(II). This ribosomal storage accounts for millimolar amounts of intracellular Zn(II). In Chapters 3 and 4 studies on several ribosomal proteins (L31, L13, L22, L24, and L29) are presented in an effort to identify Zn(II) binding proteins that could transfer Zn(II) to nascent proteins. Our data show that soluble L31 adopts a unique Zn(II) binding motif containing one cysteine and histidine. This Zn(II) binding site is reminiscent of the Cu(I) binding site of ATX1, a copper metallochaperone. Close examination of the *E. coli* ribosome crystal structures shows that L31 does not bind Zn(II) with the same binding site as in solution. By accounting for all known data about Zn(II) homeostasis in *E. coli*, it is hypothesized that ribosomal protein L31, while in solution and not bound to the ribosome, acts as a Zn(II) metallochaperone, delivering Zn(II) to nascent proteins as they exit the ribosome.

ZINC HOMEOSTASIS IN *E. COLI*

A Dissertation

Submitted to the Faculty of
Miami University in partial
Fulfillment of the requirements
For the degree of
Doctor of Philosophy
Department of Chemistry and Biochemistry

by

Mart Patrick Hensley
Miami University
Oxford, Ohio
2011

Dissertation Director: Dr. Michael W. Crowder

Table of Contents

List of Tables iv

List of Figures v

Chapter 1: Introduction

1.1 The Chemistry of Zinc in Biology 1

1.2 Zn(II) Homeostasis in Eukaryotes 3

1.3 Zn(II) Homeostasis in Prokaryotes 5

1.4 A New Model for Zn(II) homeostasis in *E. coli* 9

1.5 References 14

Chapter 2: Elemental and spectroscopic analysis of 70S *E. coli* ribosomes

Summary 18

2.1 Introduction 18

2.2 Material and Methods 18

2.2.1 Growth of cells 18

2.2.2 Preparation of ribosomes by centrifugation 19

2.2.3 Preparation of Zn(II)- and EDTA-treated ribosomes 19

2.2.4 In vitro transcription/translation 19

2.2.5 Elemental analyses 20

2.2.6 Extended X-ray absorption fine structure spectroscopy 20

2.3 Results 21

2.4 Discussion 24

2.5 Acknowledgements 27

2.6 References 28

Chapter 3: Characterization of Zn(II)-responsive proteins

Summary 32

3.1 Introduction 32

3.2 Material and Methods 34

3.2.1 Cloning, over-expression, and purification of L31 34

3.2.2 Metal analyses 35

3.2.3 Preparation and characterization of Co(II)-substituted MBP-L31 35

3.2.4 Site-directed mutagenesis studies 36
3.2.5 L31 EXAFS studies 37
3.3 Results 38
3.4 Discussion 42
3.5 Acknowledgements 45
3.6 References 46

Chapter 4: Cloning, over-expression, purification, and elemental analysis of L13, L22, L24, and L29
Summary 48
4.1 Introduction 48
4.2 Material and Methods 49
4.2.1 Cloning, over-expression, and purification of L13, L22, and L24 49
4.2.2 Cloning, over-expression, and purification of L29 50
4.2.3 Metal analyses 51
4.2.4 In-gel trypsin digestions and MALDI-TOF mass spectra 51
4.2.5 Database analyses 52
4.3 Results 52
4.4 Discussion 57
4.5 Acknowledgements 59
4.6 References 60
Chapter 5: Conclusions
5.1 Perspectives on metal ion homeostasis in prokaryotes 61
5.2 Approaches taken 61
5.3 Future directions 66
5.4 References 72

List of Tables

2.1 Elemental analyses of *E. coli* 70S ribosomes 23
3.1 Metal analyses of MBP-L31 and mutants 39
4.1 Metal analyses of L13, L22, L24, and MBP-L29 57

List of Figures

1.1 Irving-Williams Series 3

1.2 Zn(II) Homeostasis in Eukaryotes 5

1.3 Zn(II) Homeostasis in Prokaryotes 7

1.4 Co-translational model of Zn(II) homeostasis 12

2.1 Comparsion of the EXAFS Fourier transforms of the Zn(II) depleted and supplemented *E. coli* ribosomes 24

2.2 Fourier transforms of EDTA-treated ribosomes 26

2.3 Structure of *E. coli* 30S and 50S ribosome 27

3.1 MBP-L31 SDS-PAGE gel 38

3.2 UV-Vis of Co(II)-substituted MBP-L31 40

3.3 EXAFS of Zn(II) MBP-L31 41

3.4 Crystal structure of L31 44

3.5 Crystal structure of L36 45

4.1 Purification SDS-PAGE gel of L13 53

4.2 Purification SDS-PAGE gel of L22 54

4.3 Purification SDS-PAGE gel of L24 55

4.4 Purification SDS-PAGE gel of MBP-L29 56

4.5 The exit of the polypeptide tunnel on the 50S subunit 59

5.1 Co-translational model of Zn(II) homeostasis 69

Chapter 1
Introduction

1.1 The Chemistry of Zinc in Biology

From the study of the complete genomes sequenced to date and the following primary sequences of the potential proteomes, it is estimated that one out of every three proteins requires a metal cofactor (1). Given the abundance and important structural and catalytic roles metals perform in biological systems, there must be mechanisms in place for the regulation of absorption, distribution, cellular uptake, and excretion of transition metals. These mechanisms must exist because many metal ions are essential for the viability of cells; however, these same metals are toxic if their intracellular concentrations become too high.

Several of the transition metals, such as Cu, Fe, Mn, and Co, utilized by biological systems can undergo detrimental oxidation-reduction reactions in the cell under certain conditions. The oxidation-reduction reactions induced by transition metals were first described by Fenton (2). To understand Fenton chemistry one must understand aerobic respiration. Aerobic organisms reduce oxygen to water in order to produce ATP (2). This process occurs through a series of coupled proton and electron transfer reactions. A small percentage of oxygen consumed is reduced incompletely to form superoxide ($O^{\cdot 2-}$). Enzymes (superoxide dismutases) have evolved to catalyze the disproportionation of superoxide to hydrogen peroxide (H_2O_2) (2). Fenton chemistry is the reaction of a reduced transition metal (Fe(II)) with an oxidant (H_2O_2) to produce very reactive radical species, for example a hydroxyl radical ($^{\cdot}OH$).

$$Fe(II)_{(aq)} + H_2O_{2\,(aq)} \Rightarrow Fe(III)_{(aq)} + 2\ {}^{\cdot}OH_{(aq)}$$

This equation presents Fenton chemistry in its simplest incarnation, though there can be many variations of this reaction (2). The very reactive radicals and other reactive oxygen species can then react with proteins, DNA, and small molecules within the cell. Specifically with amino acids, the oxidation induced by these reactive oxygen species could involve the conversion of histidine residues to asparagines residues, proline residues to glutamic semialdehyde and to pyroglutamic or glutamic acid residues, arginine residues to glutamic semialdehyde residues, or many other possibilities (3, 4). This oxidative damage has been linked to many disorders, such

as cancer, Alzheimer's disease, and Parkinson's disease (5-10). Oxidative damage is generally lumped into the amorphous term "oxidative stress". It is ironic that the redox activities of some transition metals if left unregulated can severely damage the cell, while Nature uses these same redox properties to catalyze some of the most difficult and important biochemical reactions. For example the FeMo cofactor in the nitrogen-fixing enzyme nitrogenase can perform the 8 electron reduction of N_2 into 2 molecules of NH_3, and the tetranuclear Mn cluster in the oxygen evolving complex of photosystem II can perform the 4 electron reduction of O_2 into 2 molecules of water.

Zinc is the second most abundant transition metal found in biological systems after iron (11). If one was to subtract the iron found in hemoglobin, then zinc would be the most abundant transition element found in humans and many other eukaryotes. Current estimates predict that roughly 10% of the human genome is comprised of proteins that could bind zinc (12). Zinc in biology is always in the +2 oxidation state due to the loss of two 4s electrons from its outer shell. Zn(II) is a catalytic cofactor in at least one enzyme from all six major classes of enzymes, which include oxidoreductases (oxidation-reduction reactions), transferases (transfers of functional groups), hydrolases (hydrolysis reactions), lyases (group eliminations to form double bounds), isomerases (isomerization reactions), and ligases (bond formations coupled with ATP hydrolysis) (13,14). Generally in a catalytic role Zn(II) acts as a Lewis acid, activating substrates or small molecules. This activation often involves the polarization of chemical bonds, and in the case of water, the polarization of the O-H bond lowers the pK_a of the proton resulting in the formation of a potent nucleophile (Zn(II)-OH) at neutral pH. Another common role for Zn(II) in catalytic sites is the stabilization of anionic reaction intermediates. The electrophilic nature (Lewis acidity) of Zn(II) pulls electron density from anionic intermediates effectively lowering the activation energy of some chemical reactions.

While Zn(II) can perform these catalytic roles, it always remains in the +2 oxidation state under biological conditions. This redox stability in aqueous solution makes it an ideal structural cofactor in proteins. Non-catalytic Zn(II) is found in many proteins, including Zn(II) finger proteins and in other transcription factors (15, 16). Zn(II) does not exhibit harmful redox chemistry in biological systems; however, excess Zn(II) in cells is toxic. The Irving-Williams series can be used to describe the relative stability of metal ions (in this case divalent metal ions) when forming complexes with common ligands (in this case metal binding sites in proteins).

This series predicts that metal complexes with Mn^{+2}, for example, are less stable than those with Ni^{+2}, (see below).

$$Ba^{+2}<Sr^{+2}<Ca^{+2}<Mg^{+2}<Mn^{+2}<Fe^{+2}<Co^{+2}<Ni^{+2}<Cu^{+2}>Zn^{+2}$$

Weakest ⟹ Strongest

Figure 1.1 Irving-Williams series

Due to the relative effective nuclear charges (ionic radii) and crystal field stabilization energies, Cu(II) complexes are predicted to be the most stable, followed closely by Zn(II). While the Irving-Williams series was compiled using small molecule complexes, analogies to metal centers in proteins/enzymes can be argued if we assume reversible binding of metal ions to proteins/enzymes. Therefore the Irving-Williams series predicts that Zn(II) could bind to metal binding site that would normally be occupied by other metals (17,18,19). In addition given the relatively high concentrations of Zn(II) in the biosphere, Zn(II) could bind to adventitious sites on proteins and DNA and possibly change the structure/activity of these biomolecules.

1.2 Zn(II) Homeostasis in Eukaryotes

Zn(II) homeostasis in eukaryotes has been thoroughly studied, particularly in the model organism *Sarcharomyes cerevisiae*. In *S. cerevisiae* the transcription factor Zap1 is the central player in Zn(II) homeostasis (20). Zap1 is an 880 amino acid, nuclear protein that apparently is a direct sensor of Zn(II) (20). It is responsible for the regulation of over a 100 different genes; however, the roles of all of the resulting gene products in Zn(II) homeostasis are not known.

The transcription of genes involved with Zn(II) uptake in yeast is controlled by intracellular Zn(II) levels and the Zn(II)-responsive transcription factor Zap1. Zap1 has been shown to regulate its own transcription, thereby causing an amplified response to Zn(II) levels in the cell (21). Zap1 controls the regulation of the Zn(II) import genes *ZRT1* and *ZRT2* by binding to the Zn(II)-responsive elements (ZRE's) in the promoter regions of these two genes (Figure 1.2). These genes encode Zn(II) specific transporters, which are part of the ZIP family of transporters (20). Zrt1 is a high affinity Zn(II) importer, while Zrt2 is a low affinity importer (21). Zap1 also controls Fet4, a low affinity transporter, which imports Fe(II), Cu(I), and Zn(II) into the cell (Figure 1.2) (21). Zap1 induces the activation of itself, Zrt1, Zrt2, and Fet4 under Zn(II)-limiting conditions to increase the cellular uptake of Zn(II). Interestingly, Zn(II) uptake

can also be regulated at the translational level (20). Excess Zn(II) causes Zrt1 to be ubiquitinated, which then causes the protein to be endocytosed into a vacuole. Zrt1 is the only membrane transporter known to be regulated in this way. Following transport into the cell, Zn(II) is thought to be transported to various organelles, such as Golgi, mitochondria, and nuclei or packaged into vacuoles for storage (22) (Figure 1.2).

Following import into the cell, the route Zn(II) takes to and from storage systems or organelles is unknown. In *S. cerevisiae* and many other eukaryotes Zn(II) is stored in vacuoles (Figure 1.2). Vacuoles are the only known Zn(II) storage organelles in the cytoplasm. Under high Zn(II) conditions almost 10^9 atoms of zinc/cell can be store in vacuoles (21). This vacuolar Zn(II) storage is of great utility to the cell. The transport of Zn(II) into the vacuole is accomplished by two importers, Zrc1 and Cot1 (Figure 1.2) (21). Under Zn(II)-limiting conditions, Zap1 induces the transcription of the *ZRT3* gene. Zrt3 is related to the Zrt1 and Zrt2 cellular importers (21). Zrt3 exports Zn(II) out of the vacuole and into the cytoplasm (Figure 1.2) (21). Surprisingly Zap1 also induces the expression of *ZRC1*, one of the vacuole Zn(II) importers.

It has been hypothesized that the induction of *ZRC1* gene under low Zn(II) conditions is a proactive mechanism for Zn(II) homeostasis (21). Since Zn(II) limited cells express high levels of Zn(II) importers like ZRT1, the cell is poised to accumulate large amounts of Zn(II) should it become available in the extracellular environment. This potentially rapid accumulation of Zn(II) would stress the cell. This shock is prevented by promoting the efficient transport of potential excess cytosolic Zn(II) into the vacuoles. This scenario provides the cell with a rapid protection from potentially toxic levels of cytosolic Zn(II) (21).

In low Zn(II) conditions Zn(II) conservation mechanisms are activated within the cell. Alcohol dehydrogenases (ADH's) are among the most abundant Zn(II)-binding proteins in the cell. Two genes encoding ADH isozymes, *ADH1* and *ADH3*, are repressed by Zap1 under Zn(II)-limiting conditions (21). Both of these isozymes bind two Zn(II) atoms each (21). Another ADH isozyme ADH4; however, is induced by Zap1 (21). The *ADH4* gene encodes for an ADH that is similar to an iron-dependent isozyme from *Zymomonas mobilis* (21).

There are other genes that are believed to be controlled by Zap1 that could potentially contribute to Zn(II) conservation. *ZRG17* gene encodes a protein that is involved in moving Zn(II) into the ER (21). The Zrg17 works together with Msc2, which is not regulated by Zap1,

to import Zn(II) (Figure 1.2). Another target for Zap1 regulation is UTH1 (21), which is a mitochondrial protein involved in the targeted degradation of the mitochondria by autophagy. The induction of *UTH1* by Zap1 and the subsequent degradation of the mitochondria by vacuolar enzymes could provide a source of Zn(II) for a cell under low Zn(II) conditions (21). As previously mentioned Zap1 is involved in the regulation of over 100 genes ranging from genes associated with oxidation stress tolerance, phospholipids synthesis, and sulfate assimilation (21). Future studies on the many unexplored Zap1 target genes will provide new insights into how yeast regulates Zn(II) homeostasis.

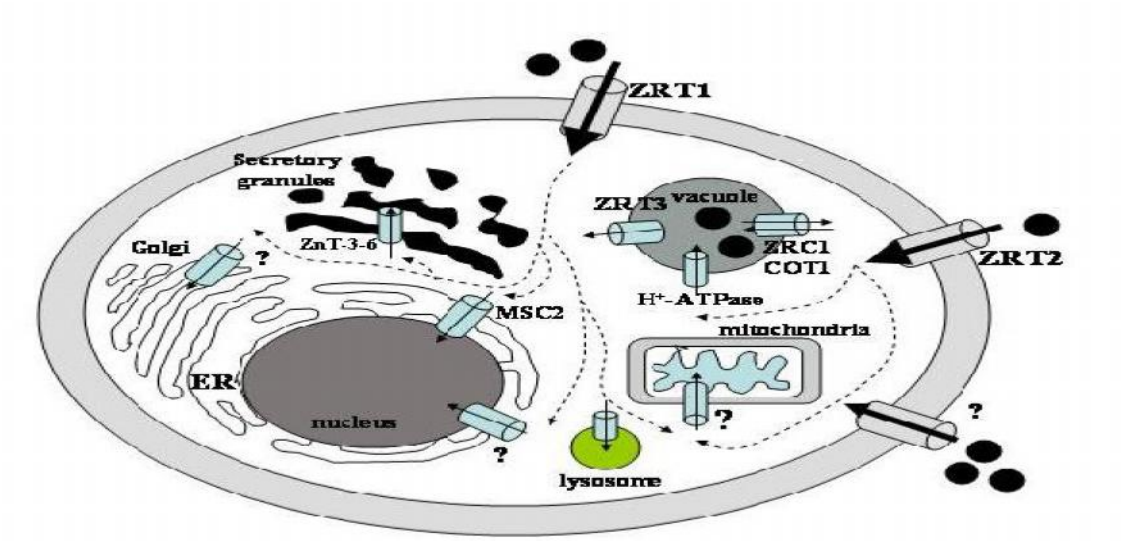

Figure 1.2 Zinc homeostasis in eukaryotes. Zinc enters the cell through 3 possible importers. Upon entering the cytoplasm, it is shuttled to various intracellular compartments via unknown mechanisms (dotted lines). Zn(II) is imported and exported from vacuoles, mitochondria, lysosomes, and nuclei and then potentially exported from the cell via secretory granules.

1.3 Zinc Homeostasis in Prokaryotes

While Zn(II) transport and homeostasis is relatively well understood in eukaryotes, Zn(II) homeostasis in prokaryotes is not. Metal ion homeostasis has been most extensively studied in *E. coli* (12, 23) and *B. subtilis* (24), and like in eukaryotes, the intracellular levels of all metal ions must be maintained at optimal concentrations. Total Zn(II) concentrations in *E. coli* cells

have been reported by O'Halloran and others to be *ca*. 2 x 10^5 atoms per cell (millimolar concentrations) (25, 26, 27). It was thought by many that there existed pools of "free" (*i.e.*, readily available) Zn(II) in the cytoplasm of cells. By using a transcription factor-based assay, O'Halloran's group showed that the concentration of "free" Zn(II) in the cell at equilibrium is 10^{-15} M, which is about one free atom of Zn(II) per cell (24). O'Halloran attempted to identify all of the Zn(II)-binding proteins and their copy numbers to account for the millimolar concentrations of Zn(II); however, only 12% of this Zn(II) could be accounted for. Unlike eukaryotes, prokaryotes do not have subcellular organelles for storing of unbound Zn(II). It is not clear how Zn(II) is distributed and stored in the cytoplasm of prokaryotic cells.

Nonetheless, much is known about the transport of Zn(II) across the cell membrane. Currently, there are three known export systems and two known import systems for Zn(II) in *E. coli* (12, 15, 28). The ZnuABC and ZupT systems are used to control uptake of Zn(II) into the cytoplasm of *E. coli* cells (Figure 1.3) (29). ZnuABC is the high-specificity Zn(II) transporter in *E. coli* and is a member of the ABC family of transporters (29). ZnuA binds to Zn(II) in the periplasm and delivers it to ZnuB, which is a transmembrane metal ion transporter, and ZnuC is an ATPase that provides the energy for Zn(II) transport across the inner membrane (Figure 1.3). The *znuABC* operon is transcriptionally-controlled by Zur, a Zn(II)-sensitive, Fur homolog transcription activator (29). ZupT is a member of the ZIP family of proteins (30) and is a low affinity Zn(II) transporter (Figure 1.3). The low affinity phosphate transporter (PitA) has been implicated in transporting Zn(II). A PitA mutant accumulates reduced amounts of Zn(II) and confers resistance to excess external Zn(II) (31). ZntA, ZitB, and YiiP are efflux pumps that remove Zn(II) from the cytoplasm of *E. coli* cells (Figure 1.3) (16, 23). ZntA is the high affinity Zn(II) exporter, while ZitB and YiiP are low affinity. The transcription of *zntA* is regulated by ZntR, a MerR homolog that up-regulates transcription as a result of Zn(II) binding (23, 25). ZitB and YiiP are members of the cation diffusion facilitator family that is reported to be regulated by Zn(II) (16, 23). It is also highly probable that there are other Zn(II) transporters in *E. coli* because double knock-out lines of the Zn(II) importers of *E. coli* (*ZnuB* and *ZupT*) are still viable and can uptake significant quantities of Zn(II) (T. Gunasekera, unpublished results). While Zn(II) import and export is well understood in *E. coli* and by analogy in other prokaryotes, cytoplasmic Zn(II) homeostasis remains unclear.

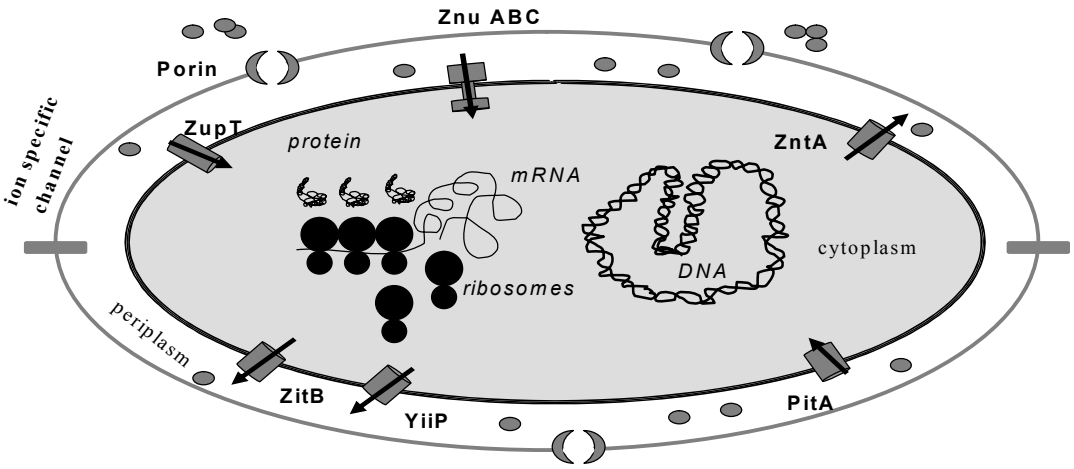

Figure 1.3 Zinc transport and homeostasis in prokaryotes. Zn(II) enters the periplasm of Gram-negative organisms via porins, and then continues on into the cytoplasm via ZnuABC, ZupT, and potentially other non-specific metal transporters such as PitA. Once in the cytoplasm, Zn(II) becomes sequestered and unavailable to the Zn(II) sensing transcription factors Zur and ZntR while simultaneously being available to proteins that require it through unknown mechanisms.

Two hypotheses have been proposed to address how cytoplasmic Zn(II) homeostasis is maintained in prokaryotes: (1) a burst model and (2) a metallochaperone model. In the burst model, low cytoplasmic levels of Zn(II) cause the rapid uptake of Zn(II) (a burst), and the Zn(II) is distributed among the millions of potential metal binding sites by relative binding affinities. Zn(II) metallation of proteins is, therefore, under thermodynamic control and equilibrium binding conditions. Conversely, excess Zn(II) would cause the rapid export of Zn(II) from the cytoplasm.

The burst mechanism of cytoplasmic Zn(II) homeostasis presents some significant questions. It is not clear how Zn(II) imported during the burst would be directed to and inserted into the correct metalloproteins, given the many potential binding sites available in the cell. In

addition, it is not clear how Zn(II) metalloproteins with relatively weak binding affinities would ever be metallated if metal binding was strictly under thermodynamic control. Importantly, the burst model of Zn(II) homeostasis is unprecedented in the literature for any metal ion, redox-active or -inactive.

The second major hypothesis developed to address intracellar Zn(II) homeostasis is a Zn(II) metallochaperone model. The Zn(II) metallochaperone model is based upon the well-established copper metallochaperones (32) and the fact that all other transition metals are transported in the cytoplasm by dedicated metallochaperones (32). Copper metallochaperones were first discovered in yeast (32). In yeast copper is brought into the cytoplasm by cell surface copper transporters, Ctr's (32). Imported copper has three potential destinations in the cell. The first is mitochondrial cytochrome c oxidase (Cytox) (32). Cytox is a key mitochondrial enzyme in the respiratory chain. Cytochrome c oxidase copper chaperone (Cox17) is a small protein that helps facilitate Cu(I) transfer to the cytochrome c oxidase with the help of two accessory factors Cox11 and Sco1 (32). The second cellular destination for copper is copper/zinc superoxide dismutase (SOD1). SOD1 helps to protect the cell by scavenging toxic superoxide anion radicals (32). The metallochaperone (CCS) for CuZn superoxide dismutase shuttles copper from Ctr to cytoplasmic SOD1. The third and final destination for copper in yeast is the Golgi (32). Copper that is delivered to the Golgi is subsequently inserted into copper enzymes destined for the cell surface or extracellular environment (32). *ATX1* (anti-oxidant) was a gene that was originally identified as an anti-oxidant when over-expressed. Later it was determined that ATX1 was shuttling copper to the Golgi (32). In yeast there are at least three specific proteins that require copper and more than three metallochaperones to shuttle this copper to those proteins.

Despite the universality of the metallochaperone model for metal ion transport, there have been no cytoplasmic Zn(II) metallochaperones yet identified in any organism. There are at least 100 Zn(II) metalloproteins in *E. coli*. If metallochaperones like those for other metal ions, transport Zn(II), there must be many distinct Zn(II) metallochaperones in *E. coli*. The inability to identify even one potential Zn(II) metallochaperone suggests that are no copper-like Zn(II) metallochaperones in *E. coli* and by extrapolation in other prokaryotes.

A recent hypothesis has addressed how cells adapt to Zn(II) starvation in *Bacillus subtilis*. In this model ribosomal protein L31 (also called RpmE), which has two putative Zn(II)-binding CXXC motifs, is replaced with the non Zn(II)-binding paralog YtiA, displacing L31 into

the cell (33, 34). Presumably L31 is degraded, and Zn(II) is released into the cell. L31 is called a C+ protein due to the presence of putative Zn(II) binding cysteine residues, and the paralog YtiA is called C- due to the absence of the same cysteine residues. YtiA, whose transcription is controlled by Zur, is not normally expressed; however, under Zn(II) limited conditions, the *ytiA* (C-) gene is up-regulated (34). There is at least one other C+/C- paralogous pair in *B. subtilis* (35). Since there are large numbers of ribosomes in *B. subtilis* as in other bacteria, the replacement of the C+ paralogs with C- paralogs would release a large amount of Zn(II) into the cytoplasm.

The *ykgM* gene, the *E. coli* equivalent to YtiA, is also under the control of Zur, the Zn(II) responsive metallo-regulatory transcription factor (36). Microarray studies of Zn(II)-limited *E. coli* cells have show that *ykgM* is one of the most up-regulated genes (37, T. Gunasekera, unpublished results). The proposed Zn(II) binding ligands present in *B. subtilis* L31 are conserved in the *E. coli* L31 (33). It is suspected that the Zn(II) starvation mechanism proposed for *B. subtilis* also operates in *E. coli*. This model only deals with the mobilization of ribosome-associated Zn(II) through the mechanism of ribosomal protein replacement under Zn(II) starvation conditions. It assumes that the ribosome binds large quanities of Zn(II). In this model a significant amount of Zn(II) could be released into the cell while ribosome function is maintained.

One of the unanswered questions about the Zn(II) starvation model is the fate of the Zn(II) once the L31 protein is released from the ribosome. The released Zn(II) would be available to bind to any potential Zn(II) sites in the cell, including to ZntR, which controls the transcription of *zntA*, the high affinity Zn(II) export pump, and Zur, which controls the transcription of *znuABC, ykgM*, and others. The same issues that were raised with the burst model would also be relevant with the Zn(II) starvation model.

1.4 A New Model for Zn(II) Homeostasis in *E. coli*.

Since none of the available models for intracellular Zn(II) transport are able to explain adequately Zn(II) homeostasis in *E. coli*, we hypothesized a new model. This model accounted for the following previously reported data: *(1)* the presence of 0.2 mM - 0.8mM Zn(II) in *E. coli* (23), *(2)* the absence of "free" Zn(II) in the cytoplasm (23), *(3)* the failure to identify any cytoplasmic Zn(II) metallochaperones in *E. coli*, *(4)* the requirement of Zn(II) for the proper

folding of many Zn(II) metalloproteins (38), *(5)* the high-specificity uptake of Zn(II) (ZnuABC) from the periplasm into the cytoplasm (12), *(6)* the high-specificity export of Zn(II) (ZntA) from the cytoplasm into the periplasm (26), and *(7)* the *in vivo* competition between L31 and YkgM binding to the ribosome in low Zn(II) conditions (in *B. subtilis*) (33, 34).

Our model proposed that the ribosome is playing a critical role in Zn(II) homeostasis. As Zn(II) enters the cell via ZnuABC, ZupT, and possibly PitA, it is bound by ribosomal proteins on the surface of the ribosome through a direct transfer from ZnuB, ZupT, and possibly PitA, to ribosomal proteins (Figure 1.4 A). Any excess "free" Zn(II) in the cytoplasm is immediately exported out of the cytoplasm by ZntA, ZitB, and YiiP. As the ribosome translates mRNA some Zn(II) metalloproteins are produced (Figure 1.4 A). These Zn(II) metalloproteins acquire Zn(II) as nascent proteins as they exit the ribosome directly from ribosomal proteins surrounding the polypeptide exit tunnel of the ribosome. The Zn(II) bound by ribosomal proteins on the surface of the ribosome is solvent-exposed with few protein ligands (Figure 1.4 B). The ribosomal protein Zn(II) ligands would be a combination of sulfur (cysteine) and nitrogen (histidine) ligands (Figure 1.4 B). The method of insertion of Zn(II) involves direct transfer from ribosomal to nascent proteins through a ligand exchange mechanism (Figure 1.4 B). The formation of a temporary complex between a ribosomal and nascent protein would be under kinetic control (Figure 1.4 B). This temporary complex allows the nascent protein time to recruit additional Zn(II) ligands. The involvement of addition nascent protein ligands in the ribosomal/nascent protein complex helps to facilitate Zn(II) transfer to the nascent protein. The identity of possible Zn(II) ligands in nascent proteins would most likely be one of three ligands, nitrogen (histidine), oxygen (glutamate/aspirate) and sulfur (cysteine), as these are the predominant Zn(II) ligands found in biological systems (39). The ribosome would become Zn(II) depleted after several rounds of Zn(II) metalloprotein translation. The ribosome would acquire more Zn(II) from the Zn(II) importers ZnuABC, ZupT, and possibly PitA.

This co-translational model addresses all current data known about Zn(II) homeostasis in prokaryotes to date. The ribosome acts as a Zn(II) cellular reservoir containing most if not all of the 0.2 mM – 0.8 mM Zn(II) in an *E. coli* cell. Ribosomal proteins act as Zn(II) metallochaperones but are not regulated by the Zn(II) metalloregulatory Zur and thus are not controlled by cytoplasmic Zn(II) levels. This explains why previous attempts to identify Zn(II) metallochaperones using Zn(II) excess and deficiency have failed to identify any to date in the

cytoplasm of prokaryotes. The delivery of Zn(II) to nascent Zn(II) metalloproteins allows Zn(II) to serve as a nucleation site for protein folding, which has been observed *in vitro* for Zn(II) proteins such as transcription factor IIIA, ADR1, and carbonic anhydrase (38). The coordination of cofactors such as Zn(II) prior to polypeptide folding maybe one of the methods that is utilized in Nature to ensure rapid formation of fully functional proteins. The kinetic control of Zn(II) metallation of nascent proteins addresses how the cell is able to metallate a wide range of Zn(II) metalloproteins with various metal binding strengths in their fully mature conformations.

With all the cellular Zn(II) residing in the ribosome, there is no "free" in the cell to possibly disrupt the high specificity uptake and export of Zn(II), which is under the control of the metalloregulatory proteins Zur and ZntR, respectively. The possible *in vivo* competition between L31 and YkgM binding to the ribosome under low Zn(II) conditions in the co-translational model is a mechanism by which the cell can draw upon the Zn(II) cellular reservoir, the ribosome, to survive during Zn(II) starvation conditions by mobilizing ribosome-associated Zn(II). The release of Zn(II)-loaded L31 from the ribosome under Zn(II) deficient conditions increases the number of Zn(II) loaded ribosomal metallochaperones participating in Zn(II) metallation of nascent proteins.

While our new Zn(II) homeostasis model is not completely tested herein, this dissertation describes experiments to test key parts of the model. In chapter 2 elemental and spectroscopic analyses of whole ribosomes were conducted to determine the Zn(II) content of whole ribosome and whether this Zn(II) was protein- or RNA-associated. The storage of Zn(II) by ribosomes is a critical aspect of our model, and co-translational binding of Zn(II) to metalloproteins would involve Zn(II) transfer from the ribosome to nascent polypeptides. We predict that proteins near the polypeptide exit site in the large subunit of the ribosome could transfer Zn(II) to polypeptides exiting the ribosome. These proteins include the universally-conserved L22, L24, and L29. These proteins were cloned, over-expressed, and characterized for Zn(II) binding (Chapter 4). We also over-expressed and purified L31 and YkgM in an effort to probe whether a Zn(II) starvation model maybe in effect in *E. coli* (Chapter 3).

The insertion of the correct metal ion into metalloproteins is essential for the activity of these proteins. Given the fact that the mechanism of insertion probably differs for pro- and eukaryotes, the understanding of this process in prokaryotes may lead to the identification of pathways that can be targeted for the generation of a new class of antibiotics. It is hoped that the

study of these metal transport mechanisms in *E. coli* will allow for homology searches for similar proteins in other strains, such as *E. coli* O157, *Yersinia pestis*, *Bacillus anthracis*, *Salmonella*, and *Shigella* species.

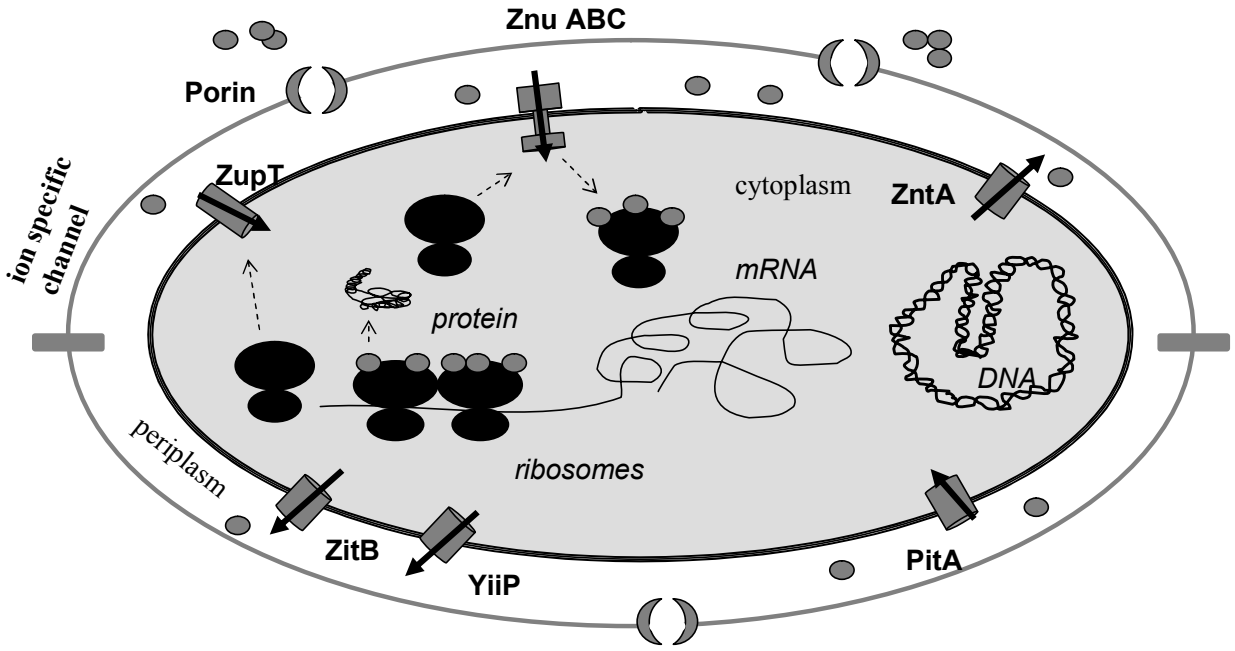

Figure 1.4 A

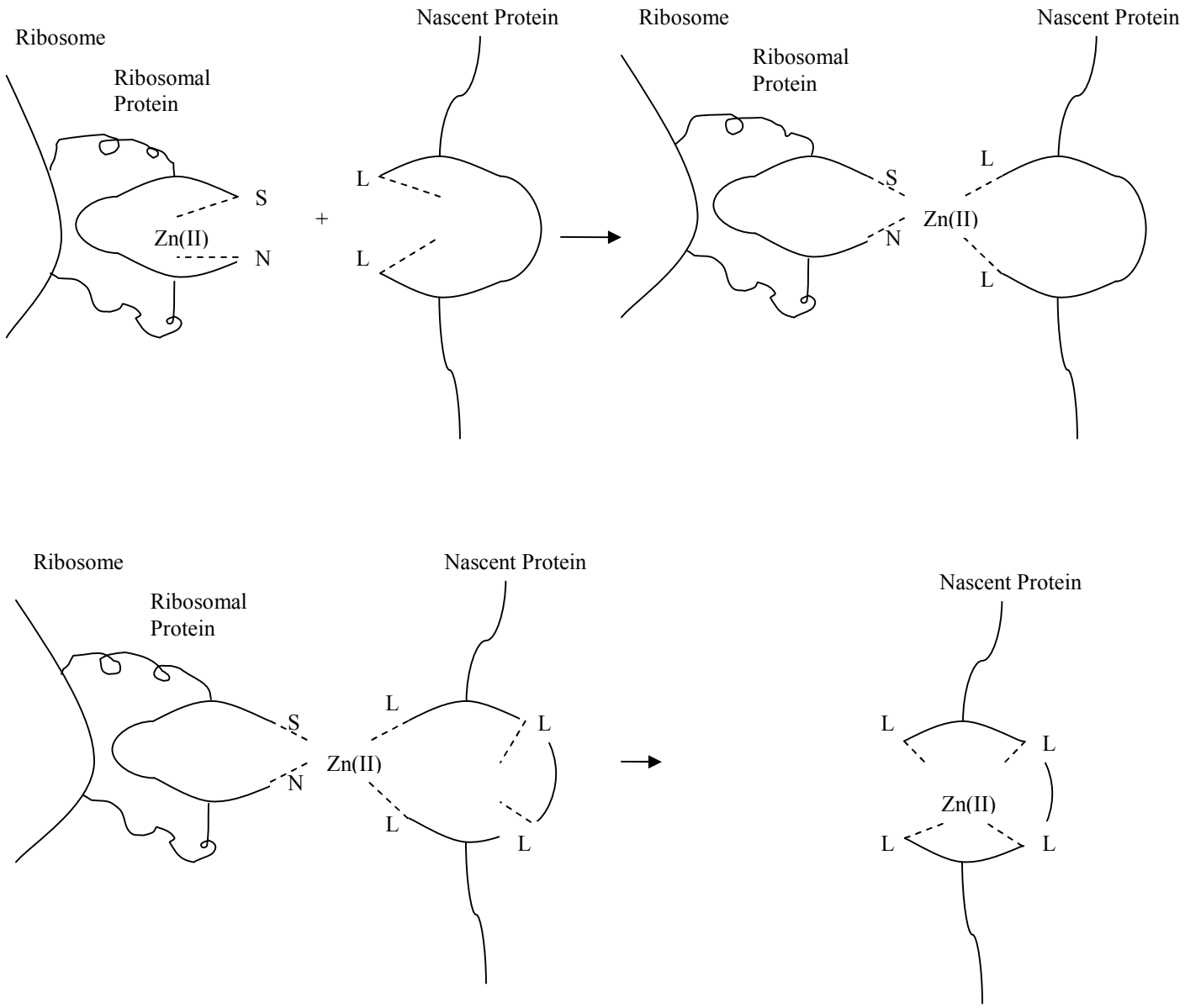

Figure 1.4 B

Figure 1.4 Co-translational model of Zn(II) homeostasis. **A**. As Zn(II) enters the cell it is bound by the ribosome by direct transfer from ZnuB, ZupT, and possibly PitA, to ribosomal proteins on the surface of the ribosome. Zn(II) is transferred from the ribosome to nascent protein by direct interaction between nascent and ribosomal proteins. Once the ribosome is depleted of Zn(II), it binds more Zn(II) from ZnuB, ZupT and possibly PitA. Any excess free Zn(II) imported into the cell is immediately exported out of the cytoplasm by ZntA, ZitB, and YiiP. **B**. The transfer of Zn(II) occurs through a ligand exchange mechanism between ribosomal and nascent proteins. A temporary complex is formed between ribosomal and nascent proteins.

1.5 References

1. Mounicou, S., Szpunar, J., and Lobinski, R. (2008) Metallomics: The concept and methodology. *Chem. Soc. Rev.* 38, 1119-1138.

2. Wardman, D., and Candeias, L. P. (1996) Fenton Chemistry: An introduction. *Radiat. Res.* 145, 523-531.

3. Farber, J. M., and Levine, R. L. (1986) Sequence of a peptide susceptible to mixed-function oxidation. Probable cation binding site in glutamine synthetase. *J. Biol. Chem.* 261, 4574-4578.

4. Amici, A., Levine, R. L., Tsai, L., and Stadtman E. R. (1989) Conversion of amino acid residues in proteins and amino acid homopolymers to carbonyl derivatives by metal-catalyzed oxidation reactions. *J. Biol. Chem.* 264, 3341-3346.

5. Stadtamn, E. R. (1986) Oxidation of proteins by mixed-function systems: Implication in protein turnover, ageing and neutrophil function. *Trends. Biochem. Sci.* 11, 11-12.

6. Oliver, C. N., Ahn, B. W., Moerman, E. J., Goldstein, S., and Stadtman, E. R. (1987) Age-related changes in oxidized proteins. *J. Biol. Chem.* 262, 5488-5491.

7. Starke-Reed, P. E., and Oliver, C. N. (1989) Proteins oxidation and proteolysis during aging and oxidative stress. *Arch. Biochem. Biophys.* 275, 559-567.

8. Stadtman, E. R. (1988) Protein modification in aging. *J. Gerontol.* 43, B112-B120.

9. Oliver, C. N., Ahn, B., Wittenberger, M. E., and Stadtman, E. R. (1985) in cellular regulation and malignant growth (Ebashi, S., ed) pp. 320-331, Japan Scientific Societies Press, Tokyo/Springer-Verlag, Berlin.

10. Oliver, C. N., Starke-Reed, P., Stadtman, E. R., Liu, G. T., Carney, J. M., and Floyd, R. A. (1990) Oxidative damage to brain proteins, loss of glutamine synthetase activity and production of free radicals during ischemia/reperfusion-induced injury to gerhil brain. *P. Natl. Acad. Sci. U.S.A*. 87, 5144-5147.

11. Patel, K., Kumar, A., Durani, S. (2007) Analysis of structural consensus of the zinc coordination centers of metalloprotein structures. *Biochim. Biophys. Acta: BBA-Proteins Proteom.* 1774, 1247-1253.

12. Hantke, K. (2005) Bacterial zinc uptake and regulators. *Curr. Opin. Microbiol.* 8, 196-202

13. Vallee, B., L., and Auld, D., S. (1990) Zinc coordination, function, and structure of zinc enzymes and other proteins. *Biochemistry.* 29, 5647-5659.

14. Vallee, B., L., and Auld, D., S. (1990) Active-site zinc ligands and activated H_2O of zinc enzymes. *P. Natl. Acad. Sci. U.S.A*. 87, 220-224.

15. Grass, G., Franke, S., Taudte, N., Niles, D., H., Kucharski, L., M., Maguire, M., E., Rensing, C. (2005) The metal permease ZupT from *Escherichia coli* is a transporter with a broad substrate spectrum. *J. Bacteriol.* 187(5), 1604-1611.

16. Lu, M., Fu, D. (2007) Structure of the zinc transporter Yiip. *Science* 317, 1746-1748.

17. Vallee, B. L., and Falchuk, K. H. (1993) The biochemical basis of zinc physiology. *Physiol. Rev.* 73, 79-118.

18. Maret, W. (2001) Zinc biochemistry, physiology, and homeostasis-recent insights and current trends. *Biometals* 14, 187-190.

19. Coleman, J. E. (1992) Zinc proteins: Enzymes, storage proteins, transcription factors and replication proteins. *Annu. Rev. Biochem.* 61, 897-946.

20. Gaither, L., A., and Eide, D., J., (2001) Eukaryotic zinc transporters and their regulations. *Biometals* 14, 251-270.

21. Eide, D., J. (2009) Homeostatic and adaptive responses to zinc deficiency. *J. Biol. Chem.* 284(28), 18565-18569.

22. Vallee, B. L., and Auld, D. S. (1995) Zinc metallochemistry in biochemistry. *Exs.* 73, 259-277.

23. Hantke, K. (2001) Bacterial zinc transportors and regulators. *Biometals* 14, 239-249.

24. Moore, C., M., and Helman, J., D. (2005) Metal ion homeostasis in *Bacillus subtilis*. *Curr. Opin. Microbiol.* 8, 188-195.

25. Outten, C., E., and O'Halloran, T.,V. (2001) Femtomolar sensitivity of metalloregulatory proteins controlling zinc homeostasis. *Science* 292, 2488-2492.

26. Banci, L., Bertini, L., Ciofi-Baffoni, S., Finnely, L., A., Outten, C. E., and O'Halloran, T., V. (2002) A new zinc-protein coordination site in intracellular metal trafficking: Solution structure of the Apo and Zn(II) forms of ZntA. *J. Mol. Biol.* 323, 883-897.

27. Finney, L., A., and O'Halloran, T., V. (2003) Transition metal speciation in the cell: Insights from the chemistry of metal ion receptor. *Science* 300, 931-936.

28. Grass, G., Fan, B., Rosen, BP., Franke, S., Niles, DH., and Rensing, C. (2001) ZitB (YbgR), a member of the cation diffusion facilitator family. Is an additional zinc transporter in Escherichia coli. *J. Bacteriol.* 183(15), 4664-4667.

29. Outten, C., E., Tobin, DA., Penner-Hahn, JE., and O'Halloran, TV. (2001) Characterization of the metal receptor sites in *Escherichia coli* Zur, an ultrasensitive Zinc (II) metalloregulatory protein. *Biochemistry.* 40(35), 10417-10423.
30. Grass, G., Wong, M., B., Rosen, BP., Smith, R., L., and Rensing, C. (2002) ZupT is a Zn(II) uptake system in *Escherichia coli*. *J. Bacteriol.* 184(3), 864-866.
31. Beard, S., J., Hashim, R, Wu, G., H., Binet, M., R., B., Hughes, M., N., and Poole, R., K. (2000) Evidence for the transport of zinc(II) ions via the inorganic phosphate transport system in *Escherichia coli. FEMS Microbiol. Lett.* 184, 231-235.
32. Robinson, N., J., Winge, D., R. (2010) Copper Metallochaperones. *Annu. Rev. Biochem.* 79, 537-562.
33. Nanamiya, H., Akanuma, G., Natori, Y., Murayama, R., Kosono, S., Kudo, T., Kobayashi, K., Ogasawara, N., Park, SM., Ochi, K., and Kawamura, F. (2004) Zinc is a key factor in controlling alternation of two types of L31 protein in the *Bacillus subtilis* ribosome. *Mol. Microbiol.* 52(1), 273-283.
34. Natori, Y., Nanamiya, H., Akanuma, G., Kosono, S., Kudo, T., Ochi, K., Kawamura, F. (2007) A fail-safe system for the ribosome under zinc-limiting conditions in *Bacillus subtilis*. *Mol. Microbiol.* 63(1), 294-307.
35. Panina, E., M., Mironov, A., A., and Gelfand, M., S. (2003) Comparative genomics of bacterial zinc regulons: Enhanced ion transport, pathogenesis, and rearrangement of ribosomal proteins. *P. Natl. Acad. Sci. U.S.A.* 100(17), 9912-9917.
36. Hemm, M., R., Paul, B., J., Miranda-Rios, J., Zhang, A., Soltanzad, N., and Storz, G. (2010) Small stress response proteins in *Escherichia coli*: Proteins missed by classical proteomic studies. *J. Bacteriol.* 192(1), 46-58.
37. Sigdel, T. K., J. A. Easton, and M. W. Crowder**.** (2006) Transcriptional response of *Escherichia coli* to TPEN. *J. Bacteriol.* 188**,** 6709-6713.
38. Cox, E., H., and McLendon, G., L., (2000) Zinc-dependent protein folding. *Curr. Opin. Chem. Biol.* 4, 162-165.
39. Krezel, A., Hao, Qiang., Wolfgang, M. (2007) The zinc/thiolate redox biochemistry of metallothionein and the control of zinc ion fluctuation in cell signaling. *Arch. Biochem. Biophys.* 463, 188-200.

Chapter 2

Elemental and Spectroscopic Analysis of 70S *E. coli* Ribosomes

M. Patrick Hensley, David L. Tierney, and Michael W. Crowder
Department of Chemistry and Biochemistry, Miami University, Oxford OH 45056

This work was funded by the National Institute of Health (GM079411 and GM093987)
This paper has been published in Biochemistry (2011) 50 9937-9939.

Professor Tierney collected and analyzed the EXAFS data presented in this chapter. The rest of the data was collected and analyzed by Patrick Hensley.

Summary

E. coli 70S ribosomes tightly bind 8 equivalents of Zn(II), and EXAFS spectra indicate that Zn(II) maybe protein-bound. Ribosomes were incubated with EDTA and Zn(II), and after dialysis, the resulting ribosomes bound 5 and 11 Zn(II) equivalents, respectively. EXAFS studies show that the additional Zn(II) in the zinc-supplemented ribosomes bind in part to the phosphate backbone of ribosome. Lastly, *in vitro* translation studies demonstrate that Zn-depleted ribosomes do not synthesize an active Zn(II)-metalloenzyme, while the as-isolated ribosomes do. These studies demonstrate that the majority of intracellular Zn(II) resides in the ribosome.

2.1 Introduction

Zinc is an essential transition metal, required for life in all organisms (1). It plays key catalytic roles in enzymes from all six major classes (2), as well as a structural role in numerous transcriptional activators and regulators (3, 4). While Zn(II) import and export is well understood (1, 5-11), surprisingly little is known about the fate of intracellular zinc. The free Zn(II) concentration within a cell has been estimated to be in the femtomolar range, while the total cellular concentration has been established as approximately 200 μM (12). However, only about 12% of the cellular Zn(II) has been accounted for as bound to Zn(II) metalloproteins (12), leaving open the question as to where the remain Zn(II) resides in the cell.

Previous studies have suggested that Zn(II) is associated with the ribosome. Atomic absorption spectroscopy of *E. coli* 70S ribosomes revealed 2 equivalents of bound Zn(II) (13), while a PAR assay of ribosomes from *B. subtilis* indicated 2.5 eq of closely-associated Zn(II) (14). Thus, while an association of zinc with the ribosome has been indicated previously, the amount of metal present in active ribosomes has not been accurately determined. Further, it has yet to be established whether ribosomal Zn(II) remains associated with the ribosome at all times, or is labile. We report here biophysical studies that indicate a possible role for the ribosome in Zn(II) storage.

2.2 Material and Methods

2.2.1 Growth of cells. *E. coli* strain BL21(DE3) was grown in 18 liters of LB broth. An overnight preculture of *E. coli* BL21(DE3) was used to inoculate 1 liter of LB in a 18 X 2 liter

flasks. The cultures were allowed to grow with shaking (200 rpm) at 37 ^{o}C until they reached an optical density at 600 nm of 1. Cells were collected by centrifugation.

2.2.2 Preparation of the ribosomes by centrifugation. *E. coli* 70S ribosomes were prepared by centrifugation (15). Bacterial cells were broken by grinding with autoclaved, levigated alumina. The lysis buffer was 20 mM Tris-HCl, pH 7.5, containing 10 mM magnesium acetate, 100 mM NH_4Cl, and 3 mM *beta*-mercaptoethanol. The broken cells were removed by centrifugation. The supernatant was then centrifuged at 45 k rpm for 3 hours at 4 ^{o} C in a Beckman L8-80M ultracentrifuge using a Beckman 80 TI to pellet the ribosomes. The ribosome pellets were then washed 4-6 times with 1 mL of lysis buffer supplemented with 500 mM NH_4Cl. The ribosome pellets were resuspended in 1 mL of lysis buffer supplemented with 500 mM NH_4Cl at 4 ^{o}C with gentle shaking for 8-12 hours. The re-suspended ribosomes were centrifuged overnight (16 hours) at 45 k rpm in Bechman 80 TI rotor with an underlay of 9 mL of the lysis buffer supplemented with 500 mM NH_4Cl and 1.1 M sucrose. Pellets were re-suspended in lysis buffer without 3 mM *beta*-mercaptoethanol and flash frozen in liquid nitrogen. Ribosomes were quantitated by using absorbance readings at 260 nm and using the conversion factor of $1A_{260}$ unit is equivalent to 23 pmol ribosomes when determined in 20 mM Tris-HCl, pH 7.5, containing10 mM magnesium acetate and 100 mM NH_4Cl. Dialysis of samples was conducted versus 2X1 liter of lysis buffer (20 mM Tris-HCl, pH 7.5, containing 10 mM magnesium acetate, 100 μM NH_4Cl, and 3 μM *beta*-mercaptoethanol) for 4 hours per dialysis.

2.2.3 Preparation of Zn(II)- and EDTA-treated ribosomes. As isolated ribosomes at a concentration of 10 μM were incubated in lysis buffer supplemented with 1000 μM of Zn(II) for one hour at 4 ^{o} C. These Zn(II)-supplemented ribosomes were then dialyzed versus 2X1 liter of lysis buffer (20 mM Tris-HCl, pH 7.5, containing 10 mM magnesium acetate, 100 mM NH_4Cl, and 3 mM *beta*-mercaptoethanol) for 4 hours per dialysis at 4 ^{o} C. As isolated ribosomes at a concentration of 10 μM were incubated in lysis buffer supplemented with 400 μM EDTA for one hour at 4^{o} C. These Zn(II)-depleted ribosomes were then dialyzed versus 2X1 liter of lysis buffer (20 mM Tris-HCl, pH 7.5, containing 10 mM magnesium acetate, 100 mM NH_4Cl, and 3 mM *beta*-mercaptoethanol) for 4 hours per dialysis at 4 ^{o} C. The dialysis tubing used had a molecular weight cutoff of 5,000.

2.2.4 In vitro transcription/translation. *In vitro* transcription/translation reactions were performed using the PURESYSTEM Classic II mini alpha kit (without ribosomes) according to

manufacturer's instructions. The *in vitro* reactions were carried out as follows 0.5 μg of plasmid DNA containing the metallo-*beta*-lactamase L1 gene (16) as well as *E. coli* 70S ribosomes up to a final concentration of 2.6 μM were added to the reactions and mixed gently. The reactions were briefly centrifuged and incubated at 37 ^{o}C for 2 hours. The reaction was stopped by placing it on ice. The whole reactions (50 μL) were added to a cuvette with nitrocefin, and the formation of the hydrolysis product of nitrocefin was monitored at 485 nm for 20 minutes. The specific activity of L1 (1.3 mmol nitrocefin hydrolyzed per second per μg of L1) was used to calculate the amount of L1 produced in the *in vitro* transcription/translation reactions. Negative controls were performed following the same procedure but without ribosomes added to the *in vitro* transcription/translation reaction. An additional, non-Zn(II)-containing enzyme, dihydrofolate reductase (DHFR), was also used in the *in vitro* translation experiments. The activity of DHFR was monitored using a dihyrofolate reductase assay kit purchased from Sigma. In brief, 25 μL of the *in vitro* translation reaction was added to a cuvette with 50 μM dihydrofolic acid, 60 μM NADPH, and 50 mM Tris-Cl, pH 7.5, and the decrease in NADPH concentration was observed at 340 nm for 5 minutes. The specific activity of *E. coli* DHFR produced in a bacterial cell free transcription-translation system has been previously reported to be 52.6 units/mg (17).

2.2.5 Elemental analyses. Ribosome samples were diluted to 50 nM with Nanopure water immediately before analysis. The metal content of each sample was determined using a PerkinElmer 7300 DV Optical Emission Spectrometer. Metal analyses were conducted in triplicate. A calibration curve was generated with the use of seven standards ranging from 1 ppb to 100 ppb of metal, and calibration curves with correlation coefficients of 0.999 or greater were used to determine the metal in each sample.

2.2.6 Extended X-ray Absorption Fine Structure Spectroscopy. Samples for extended X-ray absorption spectroscopy (XAS) (24 μM in ribosomes) were prepared with 20% (v/v) glycerol as a cryoprotectant and loaded into Lucite cuvettes with 6-μm polypropylene windows, before rapid freezing in liquid nitrogen. X-ray absorption spectra were measured at the National Synchrotron Light Source (Brookhaven National Laboratory, Upton, NY), beamline X3B, using a Si(111) double crystal monochromator; harmonic rejection was accomplished using a Ni focusing mirror. Data collection and reduction were accomplished according to published procedures (18) using E_0 = 9675 eV. The data in Figure 2.2 represent the average of the 12 scans per sample, from two independently-prepared samples each. Fourier-filtered EXAFS data were fitted utilizing

theoretical amplitude and phase functions calculated with FEFF v. 8.00 (19). The Zn-N scale factor and the threshold energy, ΔE_0, were calibrated to the experimental spectrum for *tetrakis*-1-methylimidazole zinc(II) perchlorate, $Zn(MeIm)_4$ and held fixed (at 0.78 and – 16 eV, respectively). First shell fits were then obtained for all reasonable coordination numbers, while allowing the absorber-scatterer distance, R_{as}, and the Debye-Waller factor, σ_{as}^2, for each contribution to vary.

2.3 Results

E. coli 70S ribosomes were isolated and quantified as described previously (15). To verify that the isolated ribosomes were intact and functional, *in vitro* transcription/ translation assays were performed using the PURESYSTEM Classic II mini alpha kit (20) and plasmid pUB5830 (16), which contains the gene for metallo-β-lactamase L1 from *Stenotrophomonas maltophilia*. After *in vitro* transcription/translation, the reaction mixture was assayed using nitrocefin as substrate, which indicated the production of 9.7 ± 1.9 μg of L1. Control reactions, conducted in the absence of ribosomes, did not generate metallo-*beta*-lactamase activity, demonstrating the viability of the isolated ribosomes. *In vitro* transcription/translation experiments using the kit-provided, non-Zn(II) binding dihydrofolate reductase (DHFR) gene from *E. coli* were also conducted. Theses assays revealed that 0.072 ± 0.014 μg of DHFR were produced. ICP-MS of the purified *E. coli* 70S ribosomes showed 8 equivalents of Zn(II) (Table 1). Only trace amounts of other transition metal ions, such as Co, Cu, Mn, Ni, and Fe, were present.

To examine the minimum and maximum Zn(II) content of the *E. coli* 70S ribosomes, ribosome samples were incubated with up to 100 eq of Zn(II) to fully populate weak binding sites, or up to 40 eq of EDTA to fully de-populate them, followed by exhaustive dialysis against lysis buffer (see supporting information). The concentration of Mg(II) was maintained at 10 mM throughout the incubation and dialysis steps and also during all *in vitro* transcription/translation assays. The Zn(II)-supplemented ribosomes bound 11 eq of Zn(II), while the Zn-depleted (EDTA-treated) ribosomes were found to contain only 5 eq of Zn(II) (Table 1), indicating 5 tight-binding Zn(II) sites and up to 6 weaker Zn(II) binding sites in the ribosome. *In vitro* transcription/translation reactions were conducted on the as-isolated, Zn(II)-supplemented and Zn(II)-depleted ribosomes, all of which were subjected to similar dialysis conditions, to

determine their translational activities and to evaluate whether extensive dialysis steps adversely affected their viability. Reactions with Zn(II)-supplemented ribosomes produced 5.4 ± 1.1 μg of L1 and 0.062 ± 0.012 μg of DHFR. EDTA-treated ribosomes produced no detectable L1 but produced 3.5 ± 0.6 μg of DHFR. The higher amounts of DHFR, as determined from activity assays, produced in the EDTA-treated reactions is probably due to inhibitions of DHFR activity by mono- and divalent metal cations (21). The production of no L1 in EDTA-treated reactions suggests a role of Zn(II) in the in vitro transcription/translation of this Zn(II)-metalloenzyme. Future studies will address the role of Zn(II) in ribosome activity; nonetheless, these studies demonstrate that the EDTA/Zn(II) treatments and dialysis steps did not result in inactive ribosomes.

The lower activity of the as isolated ribosomes with dialysis (1.3 μg), as compared to the as isolated ribosomes without dialysis (9.7 μg), makes it clear that the dialysis step had an adverse effect on the activity of the ribosomes, though they were still active. We surmise the lower activity of the dialyzed samples reflects the loss of loosely bound proteins from the otherwise intact ribosome, not due to loss of Mg(II), given the fact all incubation, dialysis, and *in vitro* reactions were carried out in large fold excess of Mg(II). The loss of loosely bound proteins from the surface of the ribosome and the associated destabilization upon extended dialysis of the ribosome was exasperated by pre-treated with the strong Zn(II) chelator EDTA and abolished translational activity in the Zn(II)-depleted ribosomes. The Zn(II) supplemented ribosomes with dialysis display an increase in protein production (5.4 μg) as compared to the as isolated with dialysis (1.3 μg). The Zn(II)-supplemented ribosomes are fully populated with 11 equivalents of Zn(II) bound. The presence of Zn(II) in surface associated sites on the ribosome adds stability during dialysis by mitigating the loss of loosely bound proteins from the surface of the ribosome, though the presence of additional Zn(II) was unable to recover all of the translational activity to the ribosome when compared to the as isolated ribosomes without dialysis (9.7 μg).

Table 2.1 Elemental analyses of *E. coli* 70S ribosome

50 nM Ribosomes	Zn(II) molar equivalents	Other metals (Co, Cu, Mn, Ni, and Fe) total molar equivalents
Ribosomes, as-isolated	7.9 +/- 0.1	0.52 +/- 0.30
Ribosomes, Zn(II)-treated	11.3 +/- 0.3	0.77 +/- 0.30
Ribosomes, EDTA-treated	5.0 +/- 0.1	0.77 +/- 0.30

The nature of the Zn(II) binding sites were investigated by acquiring EXAFS spectra for Zn(II)-supplemented and Zn(II)-depleted ribosomes (labeled as +Zn and –Zn in Figure 1, respectively). The two samples showed similar spectra (Figure 1, top), with the main peaks in their Fourier transforms nearly superimposable. Both samples show a single prominent outer shell feature, which moves to lower R in the Zn(II)-supplemented data. Fits to the data for Zn(II)-depleted ribosomes, representing the average of the tight binding sites, indicate a primary coordination sphere of 1 N/O donor at 1.93 Å, 3 N/O donors at 2.11 Å, and 1 sulfur donor at 2.34 Å. The outer shell feature is best modeled as a shell of 3 carbon scatterers at 3.25 Å, presumably from carboxylate ligands (Figure 1, center, and Figure S1). Any attempt to model this feature with phosphorous, as might be anticipated if the ribosomal Zn(II) were interacting with the phosphate backbone of the ribosome's constitutive RNA, was unsuccessful. In comparison, the EXAFS data for Zn(II)-supplemented ribosomes were best fit with a similar first shell of 2 N/O ligands at 1.96 Å, 3 N/O ligands at 2.14 Å and 0.5 sulfur donors at 2.29 Å. The outer shell feature, which shifts to $R + \alpha = 2.5$ Å (from 2.9 Å in the Zn(II)-depleted data), is best modeled with a mixture of 3 carbon scatterers at 3.15 Å and 1.5 phosphorous at 2.97 Å (Figure 1, bottom, and Figure S2). Both contributions appear warranted, as inclusion of the carbon shell alone leads to a 3-fold improvement in fit residual, while inclusion of the phosphorous shell alone results in more than 4-fold improvement in the fit. Inclusion of both leads to a nearly 9-fold reduction in fit residual, and their refined distances are separated by more than the 0.16 Å resolution of the data. Thus, analysis of the XAS data indicates that the Zn(II) that is tightly associated with the ribosome (Zn(II)-depleted) is most likely protein bound although we cannot rule out Zn binding to non phosphate ligands of RNA that are buried or regions of interface between protein and RNA non phosphate ligands. However, there are at least some fraction of the more loosely

associated Zn(II) (Zn(II)-supplemented), which interacts directly with the phosphate backbone of RNA.

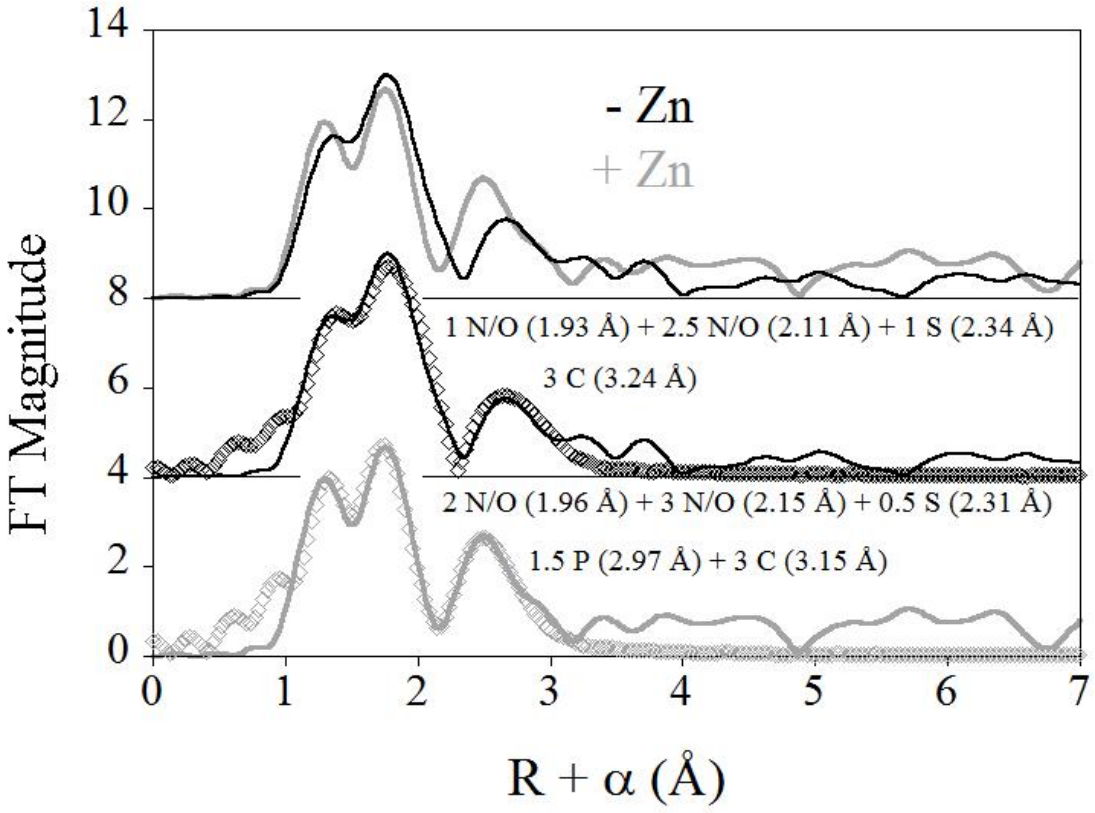

Figure 2.1 Comparison of the EXAFS Fourier transforms for EDTA-treated (-Zn, solid black line) and Zn(II)-treated (+Zn, solid gray line) *E. coli* ribosomes (top), and the corresponding best fits (open symbols).

2.4 Discussion

The number of ribosomes present in an *E. coli* cell is, not surprisingly, dependent upon its growth stage. The number of ribosomes present has been estimated to fluctuate from 2,000 per cell at low growth to 70,000 at rapid growth (22). Given the average volume of an *E. coli* cell, approximately 1.8 femtoliters, (12) the present studies allow the total ribosomal Zn(II) content to be estimated. Using the as isolated value of 8 equivalents of Zn(II) per ribosome, the concentration of Zn(II) contained within ribosomes is on average 20 μM at low growth, and 520 μM under rapid growth conditions. Estimates of total cellular Zn(II) range from 0.2 mM to 0.8

mM (12, 24). Thus, the present studies suggest that a large portion of cellular Zn(II) is contained in the ribosome.

The EXAFS analyses of 70S ribosomes identified carboxylate ligands present in the outer coordination sphere of the Zn(II) bound by the ribosome. These carboxylate ligands are found only in protein ligands rather than in nucleic acid ligands. Comparsions between Fourier transforms using carboxylate and phosphorus fits on the EDTA-treated ribosome indicate clearly that the Zn(II) is protein-associated (Figure 2.2, fourth, fifth, and sixth transforms). However the outer shell feature in the Zn(II)-treated sample, which shifts to $R + \alpha = 2.5$ Å (from 2.9 Å in the Zn(II) depleted data), is best modeled with a mixture of 3 carbon scatterers at 3.15 Å and 1.5 phosphorous at 2.97 Å (Figure 2.2, bottom). The XAS data reveal that the tightly-associated Zn(II) is most likely protein bound and that some fraction of the more loosely-associated Zn(II) interacts with the phosphate backbone of RNA.

Previous studies have suggested as many as eight ribosomal proteins that are capable of binding Zn(II) (25, 26, 27.) The *B. subtilis* ribosomal protein L31 has clearly been shown to bind Zn(II) (25). The solution structure of ribosomal protein L36 from *T. thermophilus* revealed a Zn(II)-ribbon-like fold (26), suggesting it, too, may bind Zn(II). Further proteomic studies have suggested that *E. coli* ribosomal proteins L2, L13, S2, S15, S16, and S17 could bind Zn(II) (27). Our finding that 8 Zn(II) are bound to the ribosome under normal conditions indicates that perhaps all of them bind Zn(II).

The current report supports the possible presence of four Zn(II) binding proteins in the large ribosomal subunit of the 70S *E. coli* ribosome (L36, L31, L13, and L2) and four Zn(II) binding proteins in the small subunit (S17, S16, S15, and S2) (Figure 2.3). The ribosomal associated Zn(II) identified in this study is probably serving a structural in possible protein sites in the ribosome. Further study on these potential Zn(II) binding proteins is required to validate protein binding of ribosomal Zn(II) content. Currently investigations by our group into the metal binding capabilities of isolated *E. coli* L36, L31, and L13 have indicated all these proteins are able to bind Zn(II) while isolated in solution (M. P. Hensley and M. W. Crowder, unpublished). Future studies will focus on the fate of ribosomal Zn(II) and its possible involvement in metallation of Zn(II) metalloproteins.

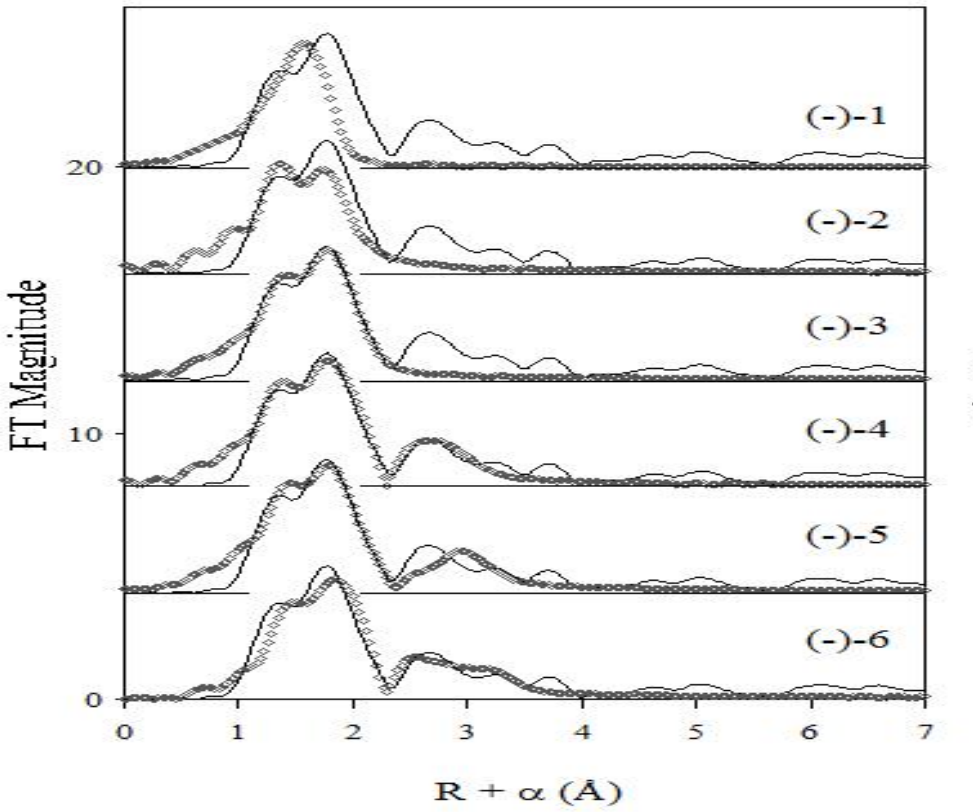

Figure 2.2 Fourier transforms of EDTA-treated ribosomes. First transform ((-)-1) 6 N/O ligands at 2.13 Å. Second transform ((-)-2) 3 N/O ligands at 2.01 Å and 3 N/O ligands at 2.18 Å. Third transform ((-)-3) 1 N/O ligand at 1.93 Å, 2.5 N/O ligands at 2.11 Å, and 1 S ligand at 2.34 Å. Fourth transform ((-)-4) 1 N/O ligand at 1.93 Å, 2.5 N/O ligands at 2.11 Å, 1 S ligand at 2.34 Å, and 3 C ligands at 3.25 Å. Fifth transform ((-)-5) 1 N/O ligand at 1.93 Å, 2.5 N/O ligands at 2.11 Å, 1 S ligand at 2.34 Å, and 1 P ligand at 3.02 Å. Sixth transform ((-)-6) 1 N/O ligand at 1.93 Å, 2.5 N/O ligands at 2.11 Å, 1 S ligand at 2.34 Å, 3 C ligands at 3.25 Å, and 1 P ligand at 3.02 Å.

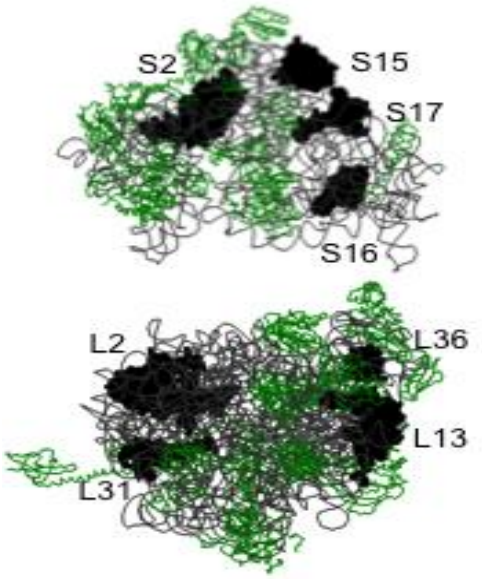

Figure 2.3 Structure of *E. coli* 30S (top) and 50S (bottom) ribosome with potential Zn(II) binding proteins labeled. This figure was rendered with Raswin using protein databank coordinates 2AVY and 2AW4C (28).

2.5 Acknowledgements

The author would like to thank Dr. Gary Janssen, Jacquelin Giliberti, and Rachel Desmone for their instruction and assistance in ribosome isolation and handling.

2.6 References

1. Hantke, K**.** (2005) Bacterial zinc uptake and regulators. *Curr. Opin. Microbiol*. 8**,**196-202.

2. Vallee, B., L., and Auld, D., S. (1995) Zinc metallochemistry in biochemistry, *Interface between and Chemistry and Biochemistry* (Joiles, P., and Jornvall, H., Eds.), pp 259-277, Birkhauser Verlag, Basel, Switzerland.

3. Andreini, C., Banci, L., Bertini, I., and Rosato, A. (2006) Zinc throughout the three domains of life. *J. Proteome Res.* 5, 3173-3178.

4. Laity, J., H., Lee, B., M., and Wright, P., E. (2001) Zinc finger proteins: new insights into structural and functional diversity. *Curr. Opin. Struct. Biol.* 11, 39-46.

5. Grass, G., B. Fan, B. P. Rosen, S. Franke, D. H. Nies, and C. Rensing**.** (2001) ZitB(YbgB), a member of the cation diffusion facilitator family, is an additional zinc transporter in *Escherichia coli*. *J. Bacteriol.* 183**,** 4664-4667.

6. Grass, G., Franke, S., Taudte, N., Nies, D., H. Kucharski, L., M., Maguire, M., E., and Rensing. C**.** (2005) The metal permease ZupT from *Escherichia coli* is a transporter with a broad substrate spectrum *J. Bacteriol*. 187**,** 1604-1611.

7. Lu, M., and Fu. D. (2007) Sturcture of the zinc transporter YiiP. *Science* 317**,**1746-1748.

8. Brocklehurst, K., R., Hobman, J., L., Lawley, B., Blank, L., Marshall, S., J., Brown, N., L., and Morby, A., P. (1999) ZntR is a Zn(II)-responsive MerR-like transcriptional regulator of zntA in *Escherichia coli. Mol. Microbiol.* 31, 893-902.

9. Grass, G., M. Wong, D.,Rosen, B., P., Smith, R., L., and Rensing., C. (2002) ZupT is a Zn(II) uptake system in *Escherichia coli*. *J. Bacteriol.* 184 (3)**,** 864-866.

10. Patzer, S., I., and Hantke, K. (1998) The ZnuABC high-affinity zinc uptake system and its regulator Zur in *Escherichia coli*. *Mol. Microbiol.* 28, 1199-1210.

11. Patzer, S., I., and Hantke, K. (2000) The zinc-responsive regulator Zur and its control of the znu gene cluster encoding the ZnuABC zinc uptake system in *Escherichia coli*. *J. Biol. Chem*. 275, 24321-24332.

12. Outten, C. E., and O'Halloran. T., V**.** (2001) Femtomolar sensitivity of metalloregulatory proteins controlling zinc homeostasis. *Science* 292, 2488-2492.

13. Chan, Y., Suzuki, K., Olvera, J., and Wool, I., G. (1993) Zinc Finger-like motifs in rat ribosomal proteins S27 and S29. *Nucleic Acids Research*. 21(3), 649-655.

14. Gabriel, S., E., and Helmann, J., D. (2009) Contributions of Zur controlled ribosomal proteins to growth under zinc starvation conditions. *J. Bacteriol.*. 191(19),6116-6122.
15. Spedding, G. **(**1990) Isolation and analysis of ribosomes from prokaryotes, eukaryotes and organelles. *Ribosome and Protein Synthesis: A practical approach*. Pp 1-29. IRL press Oxford UK.
16. Crowder., M., W., Walsh, T., R., Banovic, L., Pettit, M., and Spencer, J. (1998) Overexpression, purification, and characterization of the cloned metallo-ß-lactamase L1 from *Stenotrophomonas maltophilia*. *Antimicro. Agents. and Chemo*. 42, 921-926.
17. Mouat., M., F. (2000) Dihydrofolate influences the activity of *Escherichia coli* dihydrofolate reductase synthesized *de novo*. *Int. J. Biochem. Cell Biol.* 32, 327.
18. Costello, A.., Periyannan, G., Yang, K., W., Crowder, M., W., andTierney, D., L. (2006) Site-selective binding of Zn(II) to metallo-*beta*-lactamase from *Stenotrophomonas maltophilia*. *J. Biol. Inorg. Chem.* 11, 351-358.
19. Ankudinov, A., L., Ravel, B., Rehr, J., J., and Conradson, S., D. (1998) Real-space multiple-scattering calculation and interpretation of x-ray-absorption near-edge structure. *Phys. Rev. B*. 58, 7565-7576.
20. Shimizu, Y., Inoue, A., Tomari, Y., Suzuki, T., Yokogawa, T., Nishikawa, K., and Ueda., T**.** (2001) Cell-free translation reconstituted with purified components. *Nature Biotech*. 19, 751-755.
21. Baccanari, D., Phillips, A., Smith, S., O., Sinski, D., and Burchall, J. (1975) Purification and properties of *Escherichia coli* dihydrofolate reductase. *Biochemistry.* 14, 5267-5273.
22. Kaczanowska, M., and Ryden-Aulin., M. (2007) Ribosome biogenesis and the translation process in *Escherichia coli*. *Microbiol. and Mol. Biol. Reviews*. 71(3), 477-494.
23. Moore, P., B., and Steitz, T., A. (2003) The structural basis of the large ribosomal subunit function. *Annu. Rev. Biochem*. 72,813-850
24. Eide, D., J. (2006) Zinc transporters and the cellular trafficking of zinc. *Biochim. Biophys. Acta.* 1763, 711-722.
25. Nanamiya, H., Akanuma, G., Natori, Y., Murayama, R., Kosono, S., Kudo, T., Kobayashi, K., Ogasawara, N., Park, S., M., Ochi, K., and Kawamura. F. (2004) Zinc is a key factor in controlling alternation of two types of L31 protein in the *Bacillus subtilis* ribosome. *Mol. Microbol*. 52(1), 273-283.

26. Hard, T., Rak, A., Allard, P., Kloo, L., and Garber, M. (2000) The solution structure of ribosomal protein L36 from *Thermus thermophilus* reveals a Zn-ribbon-like fold. *J. Mol. Biol*. 296, 169-180.
27. Katayama, A., Tsujii, A., Wada, A., Nishino, T., and Ishihama. A. (2002) Systematic search for zinc-binding proteins in *Escherichia coli*. *Eur. J. Biochem*. 269, 2403-2413.
28. Schuwirth, B., S., Borovinskaya, M., A., Hau, C., W., Zhang, W., Vila-Sanjurjo, A., Holton, J., M., and Cate, J., H., D. (2005) Structures of the Bacterial Ribosome at 3.5 Ä Resolution. *Science.* 310, 827-834.

Chapter 3

Characterization of Zn(II) responsive proteins in *E. coli*

M. Patrick Hensley, J. Allen Easton, David L. Tierney, and Michael W. Crowder
Department of Chemistry and Biochemistry, Miami University, Oxford OH 45056

This work was funded by the National Institute of Health (GM079411 and GM093987)
This paper was accepted for publication in the Journal of Inorganic Biochemistry (2011).

Professor Tierney collected and analyzed the EXAFS data presented in this chapter. Dr. Allen Easton cloned, over-expressed, purified and characterized MBP-YkgM. The rest of the data was collected and analyzed by Patrick Hensley.

Summary

In an effort to better understand Zn(II) transport in *E. coli*, studies were conducted to establish evidence for a Zn(II) starvation model first identified in *B. subtilis* (1). This model describes the replacement of Zn(II) binding ribosomal proteins (C+) with non Zn(II) binding ribosomal proteins (C-) under low Zn(II) conditions to mobilize ribosome-associated Zn(II) while still maintaining ribosome function. A C+/C- paralogous pair of ribosomal proteins (L31/YkgM) was identified in *E. coli* from previous genomic studies (1). L31 (C+) was cloned, over-expressed, purified, and characterized, and YkgM (C-) was over-expressed, purified, and analyzed for Zn(II) content.. L31 binds 1.2 equivalents of Zn(II), while YkgM binds no Zn(II). Spectroscopic and mutagenesis studies on L31 demonstrate that the Zn(II) binding motif of L31 contains one cysteine, one histidine, and two to three non histidine N/O ligands. An examination of previous crystal structures of the *E. coli* ribosome reveal that when L31 is bound to the ribosome there is a disruption of a potential Zn(II) site utilizing a four cysteine motif (2,3). While the results found herein do not conclusively prove the existence for a C+/C- model in *E. coli*, they do warrant further investigation.

3.1 Introduction

In an effort to better understand zinc trafficking, several groups have reported proteomic and cDNA microarray experiments to study the effects of Zn(II) excess and deficiency on *E. coli* (4,5,6,7) and to identify Zn(II) responsive proteins/genes. The rationale for these studies is that the expression levels of genes/proteins involved in Zn(II) homeostasis would be affected by cytoplasmic Zn(II) levels. When comparing previous genomic/proteomic experiments however, major differences in growth media and stress times are evident. Lee used glycerophosphate containing minimal medium (5), while Yamamoto and Brocklehurst used Luria-Bertani medium (4,7) to study Zn(II) excess conditions. Sigdel used a chemically-defined minimal medium to study Zn(II) deficient conditions (6). Stress times varied from 5 minutes by Yamamoto (7), 5 hours by Sigdel (6), and overnight batch cultures by Brocklehurst (4). All of these differences have resulted in many differentially-expressed genes being reported, and there is little or no overlap of genes found in the four studies. It has recently been shown that the proteomic profile of Zn(II)-stressed *E. coli* cells changes over time (8). It is unquestionable that gene expression is

also time-dependent and that some genes possibly involved in Zn(II) homeostasis were missed due to the incorrect choice of time to harvest the cells after stress for microarray studies.

Gunasekera and Easton (unpublished work) recently conducted a study to determine the optimal time for Zn(II)-induced transcription in an effort to identify Zn(II) responsive genes that may have be missed by previous studies. Using quantitative real-time polymerase chain reaction (qPCR), the time dependent expression levels of all genes predicted to be involved with Zn(II) homeostasis were monitored. Several Zur-regulated genes (*znuA, ykgM, yodA*) were up-regulated as much as 1000-fold over control after 30 minutes of stress, while the levels of other, non Zur-regulated genes (*zupT, zntA, zitB*) as well as 16S RNA did not change. The optimum time of stress was used to refine and enhance the subsequent cDNA array studies (Gunasekera, unpublished). These studies revealed that *znuA*, *yodA*, and *ykgM* were up-regulated by 4000-, 1200-, and 320- fold, respectively, when *E. coli* were subjected to Zn(II)-deficient conditions using the metal chelator N,N,N,N-*tetrakis*(2-pyridylmethyl)ethylenediamine (TPEN). These same genes were the most up-regulated in previous studies from the same group when the cells were harvested after 5 hours of exposure to TPEN (6). More recent studies by Graham (9) used continuous defined cultures and a Zn(II) deficient growth medium, and these results only found nine Zn(II) responsive genes that were up-regulated greater than 2-fold. *ZnuA* (2.9-fold), *yodA* (8.0-fold) and *ykgM* (2.6-fold) were among the nine (9).

YkgM protein is thought to be a paralog of the ribosomal protein L31. YkgM consists of 87 amino acids with a molecular weight of 9,920 Da and a calculated isoelectric point of 9.32 (http://www.ecogene.org). Its function in *E. coli* is unknown. The *ykgM* gene is regulated by Zur, a Zn(II) metallo-regulator, which regulates cellular Zn(II) uptake (10). While the function of YkgM in *E. coli* is unknown, a role has been proposed for a similar protein in *B. subtilis.* In *B. subtilis* ribosomal protein L31 and its paralog protein YtiA have recently been hypothesized to participate in a Zn(II) starvation model (11). Under Zn(II) limiting conditions, the Zn(II) binding ribosomal protein L31 (called C+ because it is thought to bind Zn(II) with at least two cysteine residues) is replaced with the non Zn(II) binding paralog YtiA (called C- that lacks the CXXC motif found in L31) (11,12). The replacement of L31 with YtiA is thought to mobilize ribosome-associated Zn(II), by releasing the Zn(II)-loaded L31 into the cell that is then degraded, thereby releasing Zn(II) (11). In this model a significant amount of Zn(II) is released into the cell, and

ribosome function is maintained. This Zn(II) starvation model suggests that the ribosome may serve as a possible active participant in Zn(II) homeostasis.

Analysis of amino acid sequences shows that the proposed metal binding ligands present in *B. subtilius* L31 are also present in *E. coli* L31 (1). *E. coli* L31 was cloned, over-expressed, purified, and subjected to elemental analyses. The data show that L31 binds 1.2 equivalents of Zn(II) and that YkgM binds no Zn(II) (Easton unpublished). Spectroscopic and mutagenesis studies on L31 demonstrate that the Zn(II) binding motif of L31 in solution contains one cysteine at position 16 in the amino acid sequence, one histidine residue, and two to three N/O ligands. An examination of previous crystal structures of the *E. coli* ribosome reveal that when L31 is bound to the ribosome, there is a disruption in a potential Zn(II) binding site involving all four cysteine residues (2,3). By using previous crystal structures, another potential C+/C- paralogous pair was identified.

3.2 Materials and Methods

3.2.1 Cloning, over-expression, and purification of L31. The L31 gene was cloned from genomic *E. coli* DNA from the BL21(DE3) strain using the following forward and reverse primers: 5'- AAA AAA ACA TAT GAA AAA AGA TAT TCA CCC G -3' and 5'- AAA AAG CTT TTA TTT GCT GCC CGG GAT GT -3', respectively, and these primers introduced *Hind*III and *Nde*I restriction sites flanking the L31 gene. The resulting PCR products were digested with *Nde*I and *Hind*III and ligated into digested pIAD14 (13) to generate pIAD14-L31. The gene was verified with DNA sequencing. The over-expression plasmid for L31 was transformed into BL21(DE3) *E. coli* cells. These cells were grown in LB medium supplemented with 25 μg/mL of kanamycin at 37 ^{o}C to an OD_{600nm} of 0.8-1.0, and protein production was induced by making the cultures 0.20 mM in isopropyl-β-*D*-thiogalactopyranoside (IPTG). The cultures were shaken for three hours at 37 ^{o}C. The cells were harvested by centrifugation for ten minutes at 6,831 x g. The cell pellets were re-suspended with 20 mL of ice-cold, 20 mM Tris-Cl, pH 7.6, containing 200 mM NaCl. The cells were ruptured by three passes through a French pressure cell at 16,000 lb/in^2. The cell extract was centrifuged at 23,419 x g for 25 minutes to remove insoluble material.

The supernatant was loaded at 4 ^{o}C onto an Amylose column (16 x 20 mm), which was pre-equilibrated with 20 mM Tris-Cl, pH 7.6, containing 200 mM NaCl. Bound protein was

eluted from the column using 20 mM Tris-Cl, pH 7.6, containing 200 mM NaCl and 10 mM maltose. The fractions containing protein of the correct molecular weight were collected and concentrated using an Amicon ultrafiltration unit equipped with a YM-10 nitrocellulose membrane. The concentrated protein was flash-frozen in liquid nitrogen and stored at -80 ^{o}C until further use. The purified protein was quantitated using the absorbance at 280 nm. The molar extinction coefficient of 64,720 $M^{-1}cm^{-1}$ for MBP-L31 was calculated from the amino acid composition using the protein calculator (http://www.scripps.edu/~edputnam/protcalc.html).

3.2.2 Metal analyses. Purified protein was diluted to 20 μM with deionized water and analyzed for metal, as described below (called as-isolated samples). To create Zn(II)-loaded samples, 1 mL of 300 μM purified protein was incubated with ten equivalents of Zn(II) for thirty minutes at 4 ^{o}C, and the resulting mixture was dialyzed against 2 x 2L of 20 mM Tris-Cl, pH 7.6 containing 200 mM NaCl, for eight hours each. The Zn(II)-loaded samples were diluted to 20 μM with deionized water. The metal content of the samples was determined using a Thermo Jarrell Ash ICP-AES spectrometer, using an emission wavelength of 213.856 nm. Metal analyses were conducted in triplicate. Calibration curves were generated with the use of at least four standards, with correlation coefficients of greater than 0.999, and these calibration curves were used to determine the Fe(II), Ni(II), Mn(II), and Zn(II) content in the samples. The cobalt content in Co(II)-substituted MBP-L31 samples was determined by using a PerkinElmer AAnalyst 200 Atomic Absorption spectrometer. Four standards ranging from 1.7 - 85 μM Co were used to construct a calibration curve, which had a correlation coefficient of 0.9947.

3.2.3 Preparation and characterization of Co(II)-substituted MBP-L31. Co(II)-substituted MBP-L31 was prepared using a biological incorporation procedure (14). *E. coli* BL21(DE3) cells containing pIAD14-L31 were grown at 37 ^{o}C in chelex-treated minimum medium (14), supplemented with 25 μg/mL kanamycin until reaching an OD_{600nm} between 0.6-0.8. The cultures were made 0.2 mM in IPTG and 100 μM in $CoCl_2$ and were shaken at 200 rpm for eight hours at 15 ^{o}C (14). The cells were harvested by centrifugation for ten minutes at 6,831 x g. The cell pellet was re-suspended in 20 mL of ice-cold, 20 mM 3-morpholinopropanesulfonic acid (MOPS), pH 6.5, containing 200 mM NaCl. The cells were ruptured by three passes through a French pressure cell at 16,000 lb/in^2. The cell extract was centrifuged at 23,419 x g for 25 minutes to remove insoluble material.

The supernatant was loaded at 4 ^{o}C onto an Amylose column (16 x 20 mm), which was pre-equilibrated with 20 mM MOPS, pH 6.5, containing 200 mM NaCl. Bound protein was eluted from the column using 20 mM MOPS, pH 6.5, containing 200 mM NaCl and 10 mM maltose. Column fractions were analyzed using SDS-PAGE gels, and fractions containing proteins of the correct molecular weight were collected and concentrated using an Amicon ultrafiltration unit, equipped with a YM-10 nitrocellulose membrane. The concentrated protein was flash-frozen in liquid nitrogen and stored at -80 ^{o}C until further use.

UV-Vis spectra of 1 mM Co(II)-substituted MBP-L31 were obtained on an Agilent 5480 UV-Vis spectrophotometer at 25 ^{o}C from 300-800 nm. Fully-loaded Co(II)-substituted MBP-L31 was made by adding up to 1 equivalent of $CoCl_2$ directly to the as-isolated protein and allowing the sample to incubate for 5 minutes on ice. A difference spectrum (spectrum of fully-loaded Co(II)-substituted MBP-L31 minus the spectrum of apo MBP-L31) was obtained. The addition of more than one equivalent of Co(II) to MBP-L31 resulted in protein precipitation.

3.2.4 Site-directed mutagenesis studies. The site-directed mutagenesis of L31 was accomplished by using the Stratagene QuikChange site-directed mutagenesis kit. The site-directed mutagenesis reaction was performed as per the manufacturer's instructions. The cysteine residue present at amino acid position 16 was changed to a serine residue to produce the C16S pIAD14-L31 plasmid using the following forward and reverse mutant primers, respectively,: 5'- AAA TAC GAA GAA ATT ACT GCT AGC TCG TCT TGC GGT AAC GTA ATG -'3 and 5'- CAT TAC GTT ACC GCA AGA CGA GCT AGC AGT AAT TTC TTC GTA TTT -'3. The cysteine residue present at amino acid position 18 was changed to a serine residue to produce the C18S pIAD14-L31 plasmid using the following forward and reverse mutant primers, respectively,: 5'- GAA ATT ACT GCT AGC TGC TCT TCG GGT AAC GTA ATG AAA ATC CGC -'3 and 5'- GCG GAT TTT CAT TAC GTT ACC CGA AGA GCA GCT AGC AGT AAT TTC -'3. The cysteine residues present at amino acid positions 37 and 40 were changed to serine residues to produce the C37/40S pIAD14-L31 plasmid using the following forward and reverse mutant primers, respectively,: 5'- CTG AAC CTC GAC GTG TCG AGC AAG TCG CAC CCG TTC TTC ACT GGC -'3 and 5'- GCC AGT GAA GAA CGG GTG CGA CTT GCT CGA CAC GTC GAG GTT CAG -'3. The C16S, C18S, and C37/40S pIAD14-L31 plasmids were transformed into BL21(DE3) *E. coli*. cells using the manufacture's instructions. The mutated genes were verified by DNA sequencing.

3.2.5 L31 EXAFS studies. Samples of Zn(II)-containing L31 (~ 800-900 μM, including 20% (v/v) glycerol added as a glassing agent, were loaded in Lucite cuvettes with 6 μm polypropylene windows and frozen rapidly in liquid nitrogen. X-ray absorption spectra were measured at the National Synchrotron Light Source (NSLS), beamline X3B, with a Si(111) double crystal monochromator; harmonic rejection was accomplished using a Ni focusing mirror. Fluorescence excitation spectra for all samples were measured with a 13-element solid-state Ge detector array. Samples were held at ~ 15 K in a Displex cryostat during XAS measurements. X-ray energies were calibrated by reference to the absorption spectrum of the cobalt metal foil, measured concurrently with the protein spectra. All of the data shown represent the average of ~ 12 total scans, from two independently-prepared samples each. Data collection and reduction were performed according to published procedures (15) with E_0 set to 7735 eV for Co. The Fourier-filtered EXAFS were fitted to Equation 1 using the nonlinear least-squares engine of IFEFFIT that is distributed with SixPack. Sixpack is available free of charge from its author, Sam Webb, at http://www-ssrl.slac.stanford.edu/~swebb/sixpack.htm, and IFEFFIT is open source software available from http://cars9.uchicago.edu/ifeffit.

$$\chi(k) = \sum \frac{N_{as} A_s(k) S_c}{kR_{as}^2} \exp(-2k^2 \sigma_{as}^2) \exp(-2R_{as}/\lambda) \sin[2kR_{as} + \phi_{as}(k)] \qquad \text{(Eq. 1)}$$

In Eq. 1, N_{as} is the number of scatterers within a given radius (R_{as}, ± σ_{as}), $A_s(k)$ is the backscattering amplitude of the absorber-scatterer (*as*) pair, S_c is a scale factor, $\phi_{as}(k)$ is the phase shift experienced by the photoelectron, λ is the photoelectron mean free-path, and the sum is taken over all shells of scattering atoms included in the fit. Theoretical amplitude and phase functions, $A_s(k)exp(-2R_{as}/\lambda)$ and $\phi_{as}(k)$, were calculated using FEFF v. 8.00 (16). The scale factor (S_c) and ΔE_0 for Co-N (0.74, -26 eV) and Co-S (0.85, -26 eV) scattering were determined previously and held fixed throughout this analysis (14). Fits to the current data were obtained for all reasonable integer or half-integer coordination numbers, refining only R_{as} and σ_{as}^2 for a given shell. Multiple scattering contributions from histidine ligands were approximated according to published procedures (16), fixing the number of imidazole ligands per metal ion at half-integral values while varying R_{as} and σ_{as}^2 for each of the four combined pathways (15).

3.3 Results

As mentioned in the Introduction, YkgM is hypothesized to be a non-Zn(II) binding paralog of ribosomal protein L31. To evaluate whether L31 is in fact a Zn(II)-binding protein, the *L31* gene was ligated into pIAD14 (13), which resulted in the production of a (Maltose Binding Protein) MBP-L31 fusion protein. Attempts were made to produce L31 without the MBP tag; however, the protein was insoluble. The cleavage of MBP from L31 also resulted in an insoluble L31. The MBP tag does not bind metal and thus will not complicate any metal analysis of the MBP-L31 fusion protein.

The greatest level of over-expressed MBP-L31 was obtained by allowing the bacterial cultures to grow to an $O.D._{600nm}$ of 0.8-1.0 before induction and by inducing protein production for 3 hours at 37 ^{o}C with 0.2 mM IPTG. Recombinant MBP-L31 was obtained by using a single affinity (amylose) column, and 70 mg/L of >95% pure protein was obtained (Figure 3.1).

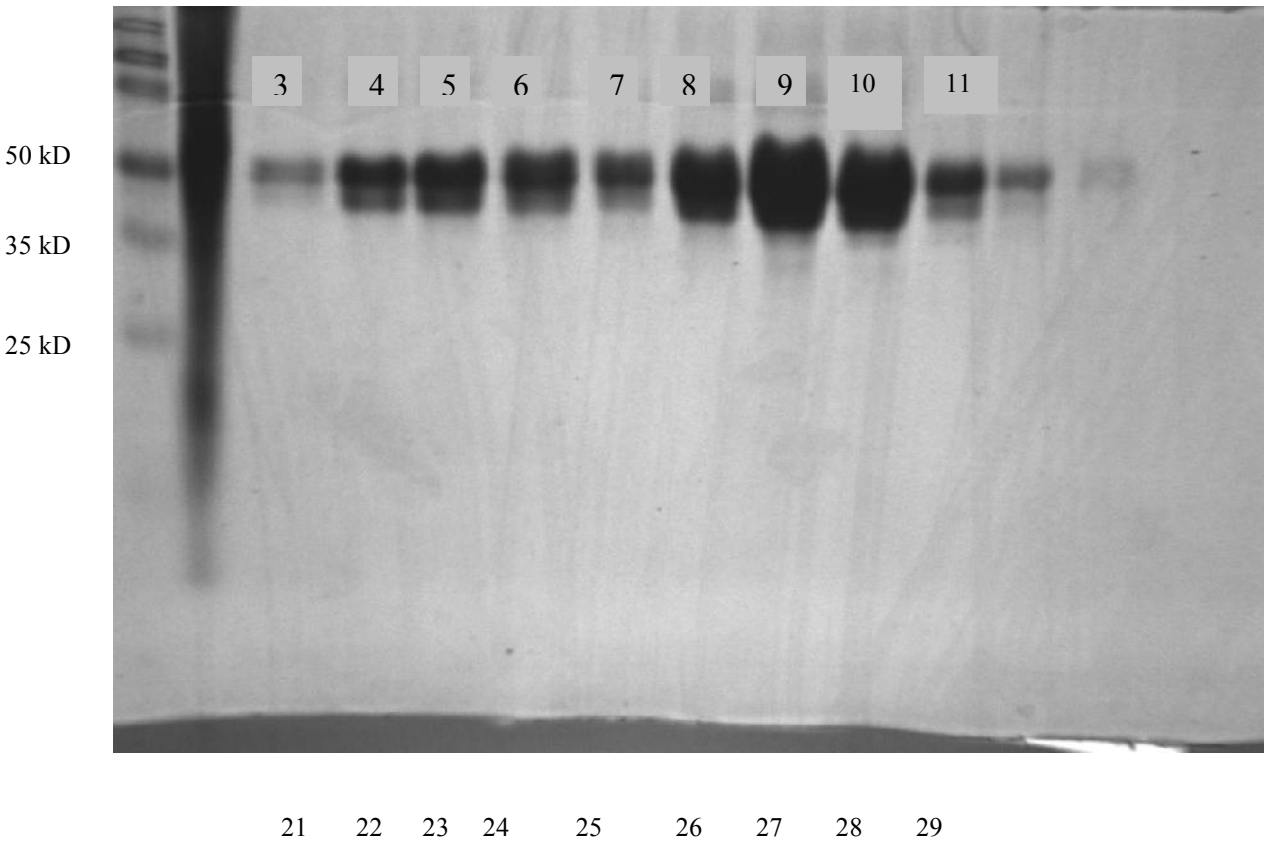

Figure 3.1. MBP-L31 SDS-PAGE Gel. Lane 1 molecular markers; Lane 2 crude MBP-L31 protein extract; Lane 3-10 purified MBP-L31 protein from Amylose column (fractions 22-29)

Elemental analyses demonstrated that MBP-L31, directly after purification, binds 0.3 $\pm$ 0.1 equivalents of Zn(II) (Table 3.1). No other metals were detected in significant amounts. To further probe for Zn(II) binding, MBP-L31 was incubated with up to 10 equivalents of Zn(II), and the resulting fusion protein was dialyzed versus 2 changes of 2 L of 25 mM Tris-Cl, pH 7.6, containing 200 mM NaCl. The resulting, metal-loaded MBP-L31 was shown to bind 1.2 $\pm$ 0.1 equivalents of Zn(II) (Table 3.1).

Table 3.1. Metal Analyses of MBP-L31 and mutants

Protein	**Zn(II) (equivalents)**
L31 as-purified	0.3 ± 0.1
L31 metal-loaded	1.2 ± 0.1
L31 (C16S) as-purified	<0.01
L31 (C16S) metal-loaded	0.4 ± 0.1
L31 (C18S) as-purified	0.03 ± 0.01
L31 (C18S) metal-loaded	1.1 ± 0.1
L31 (C37S/C40S) as-purified	0.4 ± 0.1
L31 (C37S/C40S) metal-loaded	1.3 ± 0.1

In an effort to characterize the metal binding site of MBP-L31, the Co(II)-substituted analog of MBP-L31 was prepared. A biological incorporation method (14) was utilized to produce Co(II)-substituted MBP-L31, which contained 0.2 equivalents of cobalt and 0.01 equivalents of Zn(II) as-purified. Co(II) ion was used because it is a paramagnetic structural analog of the diamagnetic Zn(II) ion. To fully load this protein with Co(II), 0.8 equivalents of Co(II) were added to the as-isolated sample. The protein precipitated if more than 1 equivalent of Co(II) was added. The electronic absorption spectrum of fully-loaded Co(II)-substituted MBP-L31 is shown in Figure 3.2. An intense band centered at 307 nm (ε = 797 M^{-1} cm^{-1}) was observed, and this feature is assigned to a cysteine sulfur ligand to metal charge transfer transition (17). Less intense features were also evident between 687 nm and 737 nm, with ε_{687nm} = 49 M^{-1} cm^{-1} and ε_{737nm} = 43 M^{-1} cm^{-1}. These latter features are assigned to ligand field transitions of high-spin Co(II) (17). The position of the ligand field transitions strongly suggest a weak ligand field around the Co(II)'s and suggests that Co(II) in MBP-L31 is bound directly to

one or more cysteine ligands. To further investigate the metal center, we attempted to obtain ^{1}H NMR spectra of the Co(II)-substituted enzyme; however, the protein precipitated during data acquisition. Efforts to stabilize the protein with low temperature acquisition were unsuccessful.

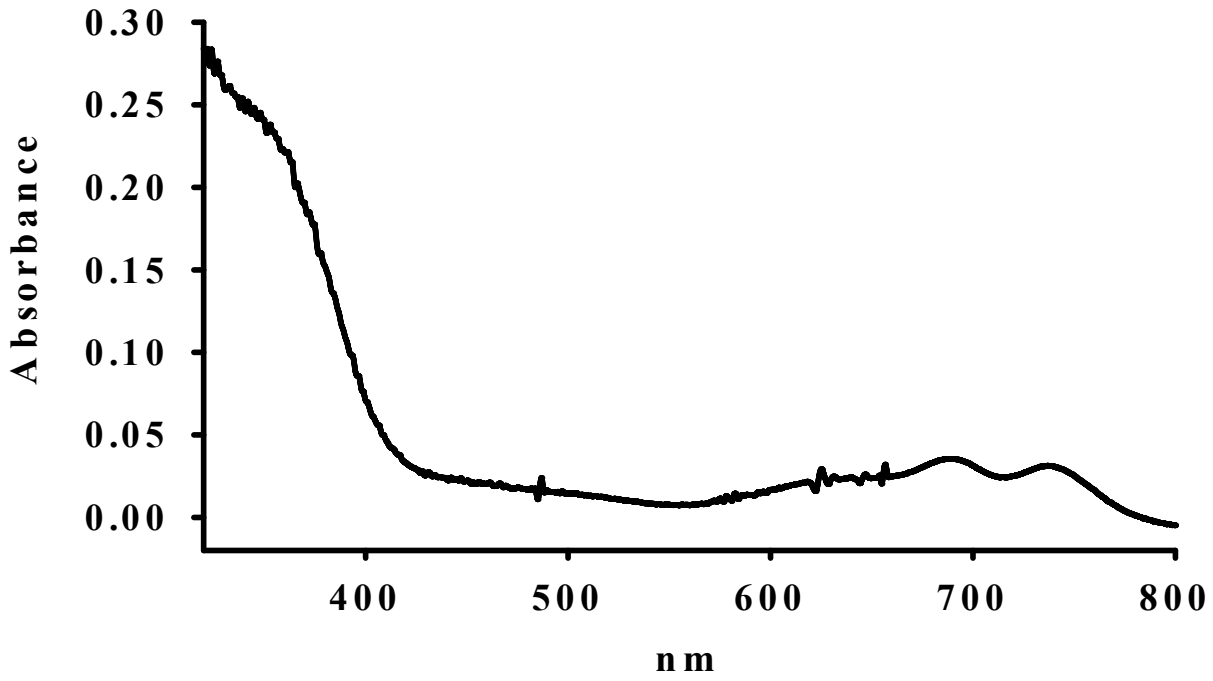

Figure 3.2. UV-Vis spectrum of 1.0 mM Co(II) substituted MBP-L31 in 20 mM MOPS, pH 6.5, containing 200 mM NaCl at 4 ^{o}C

To obtain more information about the metal binding ligands present in L31, extended X-ray absorption fine structure (EXAFS) spectroscopic studies were performed on Zn(II)-containing MBP-L31 (Figure 3.3). The top spectrum shows the experimental data in black solid line and a model (open circles) showing 4 N/O ligands in the first coordination sphere of the Zn(II) (Figure 3.3 top spectrum). Fits were greatly improved by inclusion of a sulfur ligand and retaining 3 N/O first coordination sphere ligands (Figure 3.3, middle spectrum). The fit was further improved by multiple scattering analyses that suggest 1 coordinated His, 1 Cys sulfur, and 3 additional N/O ligands (Figure 3.3, bottom spectrum).

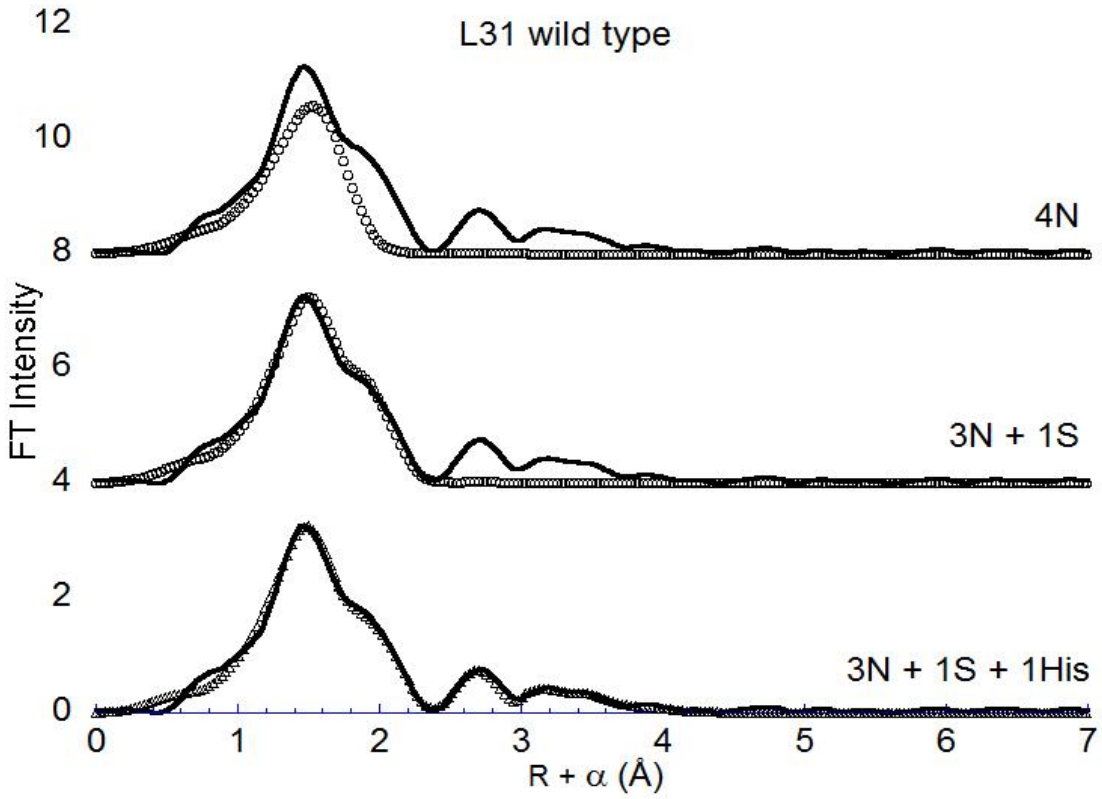

Figure 3.3. Extended X-ray Absorption Fine Structure (EXAFS) spectra of Zn(II)-containing MBP-L31. The experimental data is in black sold line and fits to the data are in open circles. The 4N, 3N +1S, and 3N+1S +1His are the simulated first shell coordination sphere surrounding the Zn(II) ion for each of the different theoretical fits.

Previous studies (11,12) in *B. subtilis* suggested that L31 binds Zn(II) using at least 2 cysteine residues in a CXXC motif, and the position of the ligand field bands in the UV-Vis spectrum of Co(II) substituted L31 from *E. coli.* suggests that one or more cysteines are bound to the metal (Figure 3.2). The EXAFS studies also predict one cysteine residue in the ligand environment for Zn(II) in *E. coli* L31. To probe for metal binding to *E. coli* L31, single amino acid mutations were introduced at cysteine 16 and 18 to generate the C16S and C18S single mutants of MBP-L31. Double amino acid mutations were introduced at cysteine 37 and 40 to generate the C37/40S double mutant of MBP-L31. All of the mutants were over-expressed, purified, and shown to be isolated as soluble fusion proteins at yields similar to those of the wild-type fusion protein. Metal analyses on the MBP-L31 mutants were conducted to probe whether any of these cysteines participate in metal binding. The as-isolated recombinant C16S mutant

contained no Zn(II) (Table 3.1). The C16S mutant was incubated with 10 equivalents of Zn(II), and the resulting protein solution was exhaustively dialyzed versus 2 changes of 2 liters of 25 mM Tris-Cl, pH 8.5, containing 200 mM NaCl. The "metal-loaded" C16S mutant contained 0.4 ± 0.1 equivalents of Zn(II) (Table 3.1). The as-isolated C18S mutant contained no Zn(II) (Table 3.1), and the "metal-loaded" C18S mutant bound 1.1 ± 0.1 equivalents of Zn(II) (Table 3.1). The as-isolated C37/40S double mutant contained 0.4 ± 0.1 equivalents of Zn(II), and the "metal-loaded" C37/40S double mutant bound 1.3 ± 0.1 equivalents of Zn(II) (Table 3.1). These results indicate that cysteine at position 16 in the amino acid sequence of L31 is the metal binding cysteine residue.

3.4 Discussion

In response to Zn(II) starvation, a Zn(II) mobilization model, called C+/C-, has been proposed in *B. subtilis*, and this model has been discussed (11,12). It has been proposed that a similar system is in place in *E. coli*, and L31(C+)/YkgM(C-) were identified as a possible paralogous pair. In support of this proposal is our recent confirmation that *E. coli* ribosome tightly binds up to 8 equivalents of Zn(II) (Chapter 2). To further support the hypothesis that a C+/C- minus system is in place in *E. coli*, we over-expressed, purified, and characterized L31.

We could only obtain soluble L31 as a fusion protein with MBP. Previous studies demonstrate that YkgM does not bind Zn(II) (A. Easton, Ph.D. dissertation). Metal analyses conducted on L31 show one equivalent of Zn(II), supporting the hypothesis that these proteins might be paralogs. Previously from the studies on RpmE/YtiA in *B. subtilis*, it was hypothesized that RpmE binds Zn(II) through 2-4 cysteine residues; these same residues are not found in the paralog YtiA and hence the name, C- protein (12). To probe whether Zn(II) binds any of the Cys residues in L31, EXAFS studies on the Zn(II)-containing L31 were conducted. The best fit to the data suggests that Zn(II) binds only 1 Cys, 1 His, and 3 N/O ligands. This result is supported by the UV-Vis data on Co(II)-substituted MBP-L31, which shows a LMCT at ~307 nm with an extinction coefficient that is consistent with only 1 Cys bound to the Co(II) (17). In addition, the site-directed mutagenesis data suggest that only Cys16 takes part in binding. The position (between 687 and 737 nm) of the ligand field transitions in the UV-Vis spectrum of Co(II)-substituted MBP-L31 suggests a very weak ligand field around the Co(II)'s (17). Given the EXAFS and mutagenesis data the position of the ligand field transitions must be due to a high-

coordinate, non-idealized geometry (square pyramid, trigonal bipyramid, or octahedral) for the Co(II) in this protein.

An examination of the crystal structure of L31 bound to the *E. coli* 50S ribosome shows that L31 binds over 100 Å from the exit tunnel (measuring the distance between Leu51 in L24 and Cys40 in L31) (Figure 3.4A) (2). Focusing on the structure of bound L31 (Figure 3.4B), the sulfur atoms in Cys37 and Cys40 are 4.4 Å apart (Figure 3.4C); however, the atoms are not facing each other perfectly for metal binding. Cys37 and Cys40 are 45 Å away from Cys16 and Cys18, which have their sulfur atoms almost 11 Å (Figure 3.4D) apart. From this structure, it is clear to see that it is impossible for all four cysteines to coordinate Zn(II) in L31 when it is bound to the ribosome. Given this structure, it would appear that Zn(II) would more likely bind in between Cys37 and Cys40; however, there is no electron density in between these cysteines in any of the *E. coli* ribosome crystal structures that were examined, possibly because of the inclusion of EDTA and high levels of Mg(II) in buffers used when purifying *E. coli* ribosomes (2). In solution, it appears that Zn(II) binds to Cys16 and possibly His30 (the closest His to Cys16 – 23 Å away) of L31. It is not clear if Zn(II) binds to the same site when L31 is bound to the ribosome. These results are not consistent with the Zn(II) starvation model in *B. subtilis* (11), which suggests that Zn(II) is bound by one or both of the CXXC motifs when the protein is bound to the ribosome (11).

When examining many crystal structures of the *E. coli* ribosome for potential Zn(II) binding sites, we discovered L36, which is a small protein that binds to the large subunit of the ribosome. Previous NMR solution studies on L36 from *T. thermophilus*, showed that Zn(II) is bound by a common Zn finger motif, consisting of Cys27, His32, Cys11, and Cys14 (Figure 3.5A) (18). In a recent structure of the *E. coli* ribosome bound to an antibiotic (3), L36 was found to bind Zn(II) even when the ribosomes were purified using high levels of EDTA. L36 was 158 Å away from the exit tunnel of the large subunit, and Zn(II) was coordinated by Cys11, Cys14, Cys27, and His33 (Figure 3.5B). Interestingly, the Zn(II) binding ligands in both structures do not point directly at the Zn(II), and the metal-ligand distances are 2.26 – 2.47 Å (see Figure 3.5). It is possible that Zn(II)/Co(II) may bind in a similar fashion to L31, resulting in a relatively weak ligand field, which would be in agreement with the ligand field transitions observed in Figure 3.2. Therefore, L36 appears to be a C+ candidate in *E. coli*. To be part of a C+/C- system however, there should be a C- paralog present in *E. coli*. A potential candidate is YkgO, which is

transcriptionally-regulated by Zur and is part of the *ykgM/ykgO* operon (10). YkgO was not identified as being Zn(II)-responsive in recent DNA microarray studies because the gene probe for YkgO was not found on the Affymetrix chips (Gunasekera, private communication). L36 has been identified as being duplicated in some bacterial genomes, *Pseudomonas aeruginosa*, *Vibrio cholerae*, and *Neisseria meningitides*, previously (1).

The evidence gathered to this point suggest strongly that in response to Zn(II) starvation *E. coli* may utilize a Zn(II) mobilization model, called C+/C-. While the results found herein do not conclusively prove the existence for a C+/C- model in *E. coli*, they do warrant further investigation. The identification of a C+/C- system in *E. coli* does not provide adequate detail on Zn(II) homeostasis. The C+/C- system simply explains how Zn(II) that is stored on the ribosome could be mobilized under Zn(II) starvation conditions; however, it does provide a foundation upon which these more intimate details of Zn(II) homeostasis can be built.

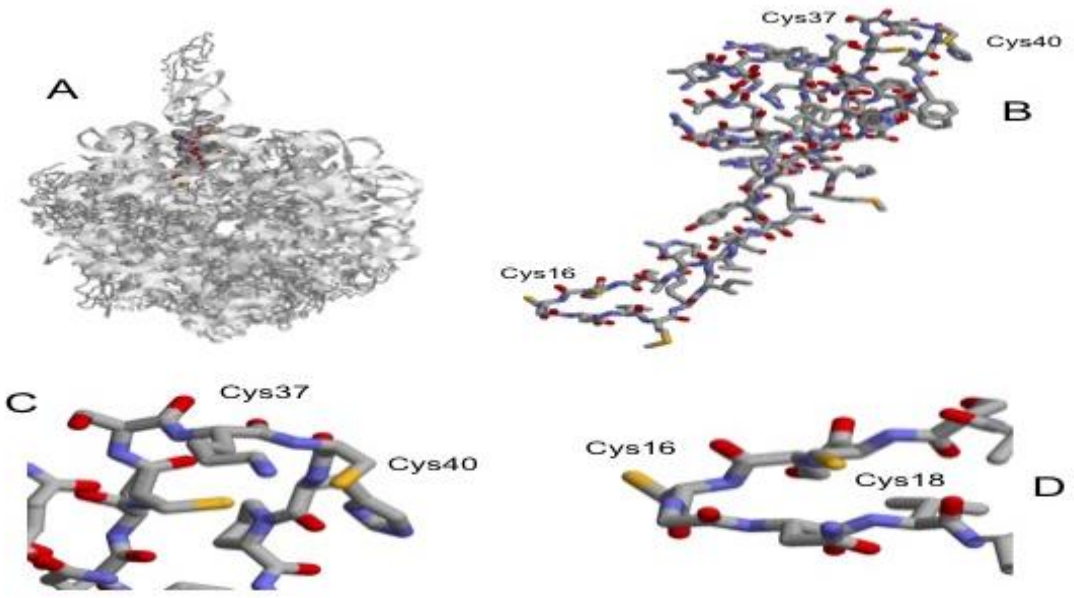

Figure 3.4 Crystal structure of L31. (A) L31 bound to *E. coli* ribosome (2). (B) *E. coli* L31. (C) Site one of L31 containing Cys37 and Cys40. (D) Site two of L31 containing Cys16 and Cys18.

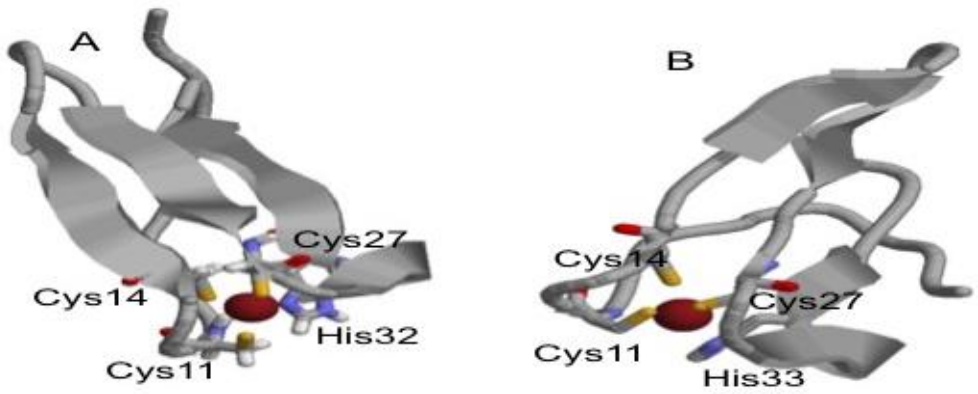

Figure 3.5 Structures of L36: (A) *T. thermophilus* L36 (NMR; (18) and (B) *E. coli* L36 (crystal structure; (3)

3.5 Acknowledgements

The author would like to thank Lauren Spadafora for her assistance in protein isolation and handling. The author would like to thank Dr. Allen Easton for his instruction on the use of Amylose column.

3.6 References

1. Makarova, K., S., Ponomarev, V., A., Koonin, E., V. (2001) Two C or nor two C: recurrent disruption of Zn-ribbons, gene duplication, lineage-specific gene loss, and horizontal gene transfer in evolution of bacterial ribosomal proteins. *Genome Biol.* 2(9), 33.1-33.14

2. Schuwirth, B., S., Borovinskaya, M., A., Hau, C., W., Zhang, W., Vila-Sanjurjo, A., Holton, J., M., Cate, J., H., D. (2005) Structures of the bacterial ribosome at 3.5 Å resolution *Science* 310, 827-834.

3. Dunkle, J., A., Xiong, L., Mankin, A., S., and Cate, J., H., D. (2010) Structure of the *Escherichia coli* ribosome with antibiotics bound near the peptidyl transferase center explain spectra of drug action. *Proc. Natl. Acad. Sci. U.S.A.* 107 (40), 17152-17157.

4. Brocklehurst, K. R., and A. P. Morby. (2000) Metal-ion tolerance in *Escherichia coli*: Analysis of transcriptional profiles by gene-array technology. *Microbiol.* 146, 2277-2282.

5. Lee, L. J., J. A. Barrett, and R. K. Poole. (2005) genome-wide transcriptional response of chemostat-cultured *Escherichia coli* to zinc. *J. Bacteriol*. 187, 1124-1134.

6. Sigdel, T. K., J. A. Easton, and M. W. Crowder. (2006) Transcriptional response of *Escherichia coli*. *J. Bacteriol*. 188, 6709-6713.

7. Yamamoto, K., and A. Ishihama. (2005) Transcriptional response of *Escherichia coli* to external zinc. *J. Bacteriol*. 187, 6333-6340.

8. Easton, J. A., P. Thompson, and M. W. Crowder. (2006) Time-dependent translational response of *E. coli* to excess zinc. *J. Biomol. Tech*. 17, 303-307.

9. Graham, A. I., Hunt, S., Stokes, S., L., Bramall, N., Bunch, J., Cox, A., G., McLead, C., W., and Poole, R., K. (2009) Severe zinc depletion of *Escherichia coli*: roles for high affinity zinc binding by ZinT, zinc transport and zinc-independent proteins. *J. Biol. Chem.* 284(27), 18377-18389.

10. Hemm, M., R., Paul, B., J., Miranda-Rios, J., Zhang, A., Soltanzad, N., and Storz, G. (2010) Small stress proteins in *Escherichia coli*: Proteins missed by classic proteiomic studies. *J. Bacteriol.* 192(1), 46-58.

11. Natori, Y., Nanamiya, H., Akanuma, G., Kosono, S., Kudo, T., Ochi, K., and Kawamura., F. (2007) A fail-safe system for the ribosome under Zn(II) limiting conditions in *Bacillus subtilis*. *Mol. Microbiol*. 63(1), 294-307.

12. Nanamiya, H., Akanuma, G., Natori, Y., Murayama, R., Kosono, S., Kudo, T., Kobayashi, K., Ogasawara, N., Park, S., M., Ochi, K., and Kawamura. F. (2004) Zinc is a key factor in controlling alternation of two types of L31 protein in *Bacillus subtilis*. *Mol. Microbol*. 52(1), 273-283.

13. McGafferty, D., Lessard I., & Walsh C. (1997) Mutational analysis of potential zinc-binding residues in the active site of the enterococcal *D*-Ala-*D*-Ala dipeptidase VanX. *Biochemistr*y. 36, 10498-10505.

14. Rajagopalan, P. T. R., S. Grimme, and D. Pei. (2000) Characterization of cobalt(II)-substituted peptide deformylase: function of the metal ion and the catalytic residue Glu-133. *Biochemistry.* 39, 779-790.

15. Costello, A.., Periyannan, G.., Yang, K., W., Crowder, M., W., and Tierney, D., L. (2006) Site-selective binding of Zn(II) to metallo-*beta*-lactamase L1 from *Stenotrophomonas maltophilia J. Biol. Inorg. Chem.* 11, 351-358.

16. Ankudinov, A., L., Ravel, B., Rehr, J., J., and Conradson, S., D. (1998) Real-space multiple-scattering calculation and interpretation of X-ray-absorption near-edge structure *Phys. Rev. B* 58, 7565-7576.

17. Holmquist B., and B. Vallee. (1979) Metal-coordinationg substrate analogs as inhibitors of metalloenzymes. *Proc. Natl. Acad. Sci. U.S.A.* 76, 6216-6220.

18. Hard, T., Rak, A., Allard, P., Kloo, L., and Garber, M. (2000) The solution structure of ribosomal protein L36 from *Thermus thermophilus* reveals a zinc-ribbon-like fold. *J. Mol. Biol.* 296, 169-180.

Chapter 4

Cloning, over-expression, purification, and elemental analyses of L13, L22, L24, and L29.

Summary

In an effort to identify Zn(II) binding proteins in close proximity to the polypeptide exit tunnel, L22, L24, and L29 were cloned, over-expressed, purified, and analyzed for Zn(II) content. None of these proteins bound significant amounts of Zn(II). The search for Zn(II) binding ribosomal proteins was expanded to include L13, which has been previously identified as a possible Zn(II) binding protein. L13 was cloned, over-expressed, purified, and analyzed for Zn(II). L13 was found to bind 0.6 molar equivalents of Zn(II).

4.1 Introduction

Previous studies on the 70S *E. coli* ribosome revealed that 8 Zn(II) ions tightly bind to as-isolated ribosomes, and EXAFS studies suggest that the Zn(II) is protein-bound (Chapter 2). Two ribosomal proteins, L31 and L36, have been shown to bind one equivalent of Zn(II) (1, 2), although it is not clear if L31 binds Zn(II) when bound to the ribosome (Chapter 3). A proteomic study was conducted looking for Zn(II) binding proteins in *E. coli* utilizing two dimensional gel electrophoresis with blotting of radioactive Zn(II) (3). In this study six ribosomal proteins L2, L13, S2, S15, S16, and S17 were identified as potentially Zn(II) binding (3); however, none of these proteins were cloned, over-expressed, purified, and evaluated for Zn(II) binding. In addition, the protocol used in this study involved the use of SDS-PAGE gels. The authors "dialyzed" the SDS and reductant out of the gel and argued that the proteins "refolded" and bound Zn(II) while still in the gel. These studies warrant the purification and metal analyses of the purified proteins. Knowledge about the precise location of Zn(II) within the ribosome may reveal information concerning the possible function of the ribosome-associated Zn(II).

In the Introduction of this dissertation, a novel model for bacterial Zn(II) homeostasis was offered. One key feature of this model was that the ribosome binds Zn(II), and this aspect has been unequivocally shown in Chapter 2. Another essential part of the model is that Zn(II) is co-translationally inserted into proteins as they exit the polypeptide tunnel. This part of the model predicts that metallation of Zn(II) metalloproteins is under kinetic control, which would

allow the successful metallation of Zn(II) metalloproteins with relatively weak binding sites. This part of the model also strongly suggests that Zn(II) would transfer from a ribosomal protein to the nascent polypeptide during translation. It is hypothesized that ribosome-associated Zn(II) would be localized near to the polypeptide exit port to facilitate transfer of Zn(II) to nascent proteins. The co-translational model predicts that Zn(II) would be bound by ribosomal proteins encircling the exit site. These include the universally-conserved L22, L24, and L29 proteins (4). The ring of proteins around the tunnel form a halo shaped platform (4). It is on this platform that the transfer of Zn(II) from the ribosome to nascent Zn(II) metalloproteins is hypothesized to occur.

In this chapter, several ribosomal proteins (L22, L24, and L29) were cloned, over-expressed, purified, and subjected to elemental analyses. None of these proteins were found to bind Zn(II). In an effort to expand the search for Zn(II) binding ribosomal proteins, L13, which was identified in the aforementioned proteomic studies (3), was over-expressed, purified, and characterized for Zn(II) binding. L13 was shown to bind 0.6 equivalents of Zn(II).

4.2 Material and Methods

4.2.1 Cloning, over-expression, and purification of L13, L22, and L24. The L13 gene was cloned from genomic *E. coli* DNA from the BL21(DE3) strain using the following forward and reverse primers for L13 5'- AAAAAAACATATGAAAACTTTTACAGCTAAA-'3 and 5' - AAAAAGCTTTTAGATGTCAAGAACTTGCG -'3, respectively. The L24 gene was cloned from genomic *E. coli* DNA from the BL21(DE3) strain using the following forward and reverse primers: 5'-AAAAAAACATATGGCAGCGAAAATCCGTC-3', and 5'-AAAAAGCTTTTACTTGATAGTTTCGCTGT-3', respectively. The L22 gene used the follow forward and reverse primer 5' - AAAAAAACATATGGAAACTATCGCTAAACA - 3' and 5' - AAAAAGCTTTCAGCGATCGGACACAACC - 3', respectively. These primers individually introduced *HindIII* and *NdeI* restriction sites flanking the L13, L22, and L24 genes. The resulting PCR products were digested with *Nde*I and *Hind*III and ligated into digested pET26B to generate pET26B-L13, pET26B-L22 and pET26B-L24. The digestion of pET26B with *HindIII* and *NdeI* removed the pelB leader sequence from the vector. The His-Tag present in the pET26B vector was not incorporated into any of the recombinant proteins. The genes were verified with DNA sequencing. The over-expression plasmids for L13, L22, and L24 were individually transformed

into BL21(DE3) *E. coli* cells. These cells were grown in LB medium supplemented with 25 μg/mL of kanamycin at 37 ^{o}C to an OD_{600nm} of 0.8-1.0, and protein production was induced by making the cultures 0.20 mM in isopropyl-β-*D*-thiogalactopyranoside (IPTG). The cultures were shaken for three hours at 37 ^{o}C. The cells were harvested by centrifugation for ten minutes at 6,827 x g. The cell pellets were re-suspended with 20 mL of ice-cold, 20 mM Tris-Cl, pH 7.5, containing 200 mM NaCl. The cells were ruptured by three passes through a French pressure cell at 16,000 lb/in^2. The cell extract was centrifuged at 23,419 x g for 25 minutes to remove insoluble material.

The L13 supernatant was treated with 5 μL of DNAase (2000U/mL) per 20 mL of crude supernatant. The supernatant was incubated at 37 ^{o}C for 15 minutes. The L13 DNAse-treated supernatant, L22 supernatant, and L24 supernatant were individually dialyzed versus 2 x 2L of ice-cold, 20 mM Tris-Cl, pH 7.5 for eight hours. The crude samples of L13, L22, and L24 were loaded at 4 ^{o}C on SP Sepharose columns (16 x 20 mm), which were pre-equilibrated with 20 mM Tris-Cl, pH 7.5. Bound protein was eluted from the column using 20 mM Tris-Cl, pH 7.6, containing 1 M NaCl. The fractions containing protein of the correct molecular weight were collected and concentrated using an Amicon ultrafiltration unit equipped with a YM-10 nitrocellulose membrane. The concentrated protein was flash-frozen in liquid nitrogen and stored at -80 ^{o}C until further use. The purified protein was quantitated using the absorbance at 280 nm. The molar extinction coefficients of 14,440 $M^{-1}cm^{-1}$ for L13 and 1,490 $M^{-1}cm^{-1}$ for L22 were calculated from the amino acid compositions using the protein calculator (http://www.scripps.edu/~edputnam/protcalc.html). Due to the lack of any aromatic amino acids, an extinction coefficient could not be calculated for L24. L24 was quantitated according to the method of Bradford (5).

4.2.2 Cloning, over-expression, and purification of L29. The L29 gene was cloned from genomic *E. coli* DNA from the BL21(DE3) *E. coli* strain using the following forward and reverse primers: 5'-AAAAAAACATATGAAAGCAAAAGAGCTGCG-3', and 5'-AAAAAGCTTTTACGCACCCGCCTTCTCG-3', respectively. These primers introduced *Hind*III and *Nde*I restriction sites flanking the L29 gene. The resulting PCR product was digested with *Nde*I and *Hind*III and ligated into digested pIAD14 (6) to generate pIAD14-L29. The gene was verified with DNA sequencing.

The over-expression plasmid for L29 was transformed into BL21(DE3) *E. coli* cells. These cells were grown in LB medium supplemented with 25 µg/mL of kanamycin at 37 ^{o}C to an OD_{600nm} of 0.8-1.0, and protein production was induced by making the cultures 0.20 mM in isopropyl-*D*-thiogalactopyranoside (IPTG). The cultures were shaken for three hours at 37 ^{o}C. The cells were harvested by centrifugation for ten minutes at 6,827 x g. The cell pellet was re-suspended with 20 mL of ice-cold, 20 mM Tris-Cl, pH 7.6, containing 200 mM NaCl. The cells were ruptured by three passes through a French pressure cell at 16,000 lb/in^2. The cell extract was centrifuged at 23,419 x g for 25 minutes to remove insoluble material.

The supernatant was loaded at 4 ^{o}C onto Amylose column (16 x 20 mm) (6), which was pre-equilibrated with 20 mM Tris-Cl, pH 7.6, containing 200 mM NaCl. Bound protein was eluted from the columns using 20 mM Tris-Cl, pH 7.6, containing 200 mM NaCl and 10 mM maltose. The fractions containing protein of the correct molecular weight were collected and concentrated using an Amicon ultrafiltration unit equipped with a YM-10 nitrocellulose membrane. The concentrated protein was flash-frozen in liquid nitrogen and stored at -80 ^{o}C until further use. The purified protein was quantitated using the absorbance at 280 nm. The molar extinction coefficient of 66,350 $M^{-1}cm^{-1}$ for MBP-L29 was calculated from the amino acid composition using the protein calculator (http://www.scripps.edu/~edputnam/protcalc.html).

4.2.3 Metal analyses. Purified protein was diluted to 20 µM with deionized water and analyzed for metal, as described below (called as-isolated samples). To create Zn(II)-loaded samples, 1 mL of 300 µM purified protein was incubated with ten equivalents of Zn(II) for thirty minutes at 4 ^{o}C, and the resulting mixture was dialyzed against 2 x 2L of 20 mM Tris-Cl, pH 7.6, containing 200 mM NaCl, for eight hours each. The Zn(II)-treated samples were diluted to 20 µM with deionized water. The metal content of the samples was determined using a Thermo Jarrell Ash ICP-AES spectrometer, using an emission wavelength of 213.856 nm. Metal analyses were conducted in triplicate. Calibration curves were generated with the use of at least four standards, with correlation coefficients of greater than 0.999, and these calibration curves were used to determine the Fe(II), Ni(II), Mn(II), and Zn(II) content in the samples.

4.2.4 In-gel trypsin digestion and MALDI-TOF MS analysis. Protein spots of the contaminate band found in the L13 SDS-PAGE gel were excised and vortexed with 100 µL of 25 mM NH_4CO_3/50% acetonitrile solutions for 10 min and then repeated twice. The same procedure was carried out for L13, L22, and L24. Gel pieces were then dried in a Speed Vac (Savant

Instruments, Holbrook, NY) and incubated overnight at 37 °C with shaking in 20 µL of 12 ng/µl trypsin in 25 mM NH_4CO_3. The supernatants from the trypsin-digests were collected in a separate tube, and the gel pieces were then vortexed with 30 µl of 50% acetonitrile/5% formic acid for 10 minutes. Supernatant from the resulting incubation was then added to the first supernatant, and this mixture was dried in a Speed Vac and re-suspended in 4 µL 50% acetonitrile/0.05% trifluoroacetic acid. Two microliters of this mixture was placed onto a matrix-assisted laser-desorption/ionization (MALDI) target. Peptide masses were collected using a Bruker Reflex III MALDI-MS instrument calibrated with angiotensin II (human, m/z = 1046.5423) and ACTH fragment 18-39 (human, m/z = 2465.1989) obtained from Sigma.

4.2.5 Database Analysis. Peptide masses determined from MALDI-TOF MS analysis were entered into ProFound (http://prowl.rockefeller.edu) and MASCOT (http://matrixscience.com) databases. Search parameters included variable modifications (cysteine as the S-carboamidomethyl derivative and methionine in oxidized form), up to 1 missed cleavage site was allowed, and at least 5 peptides representing at least a 20% sequence coverage were used as the filtering criteria for the protein identifications.

4.3 Results

To evaluate whether L13, L22, L24, and L29 are in fact Zn(II) binding proteins, the L13, L22, and L24 genes were ligated individually into pET26B, which resulted in the production of the L13, L22, and L24 recombinant proteins. We could only obtain L29 as fusion protein with Maltose Binding Protein (MBP) (6), much like our previous efforts with L31 and YkgM (Chapter 3). The L29 gene was ligated into pIAD14 (6) to generate pIAD14-L29. The greatest level of over-expression for all proteins was obtained by allowing the bacterial cultures to grow to an $O.D._{600nm}$ of 0.8-1.0 before induction and by inducing protein production for 3 hours at 37 ^{o}C with 0.2 mM IPTG. Recombinant L13, L22, and L24 were obtained by using a single SP Sepharose ion exchange column, and MBP-L29 was obtained by using a single Amylose affinity column (6).

Initially L13 proved difficult to purify, we were unable to identify the protein in any fractions that were collected off of the SP Sepharose column. It was believed that L13 was binding to DNA after cell lysis, which was producing a neutral complex. A DNase treatment of L13 was introduced after cell lysis but prior to dialysis to remove any DNA, and this step proved

successful. Approximately 50 mg per liter of L13, L22, and L24 were obtained (Figure 4.1, 4.2 and 4.3), while 70 mg per liter of MBP-L29 was obtained (Figure 4.4) using the procedures described above. The L13 fractions contained a contaminant that was identified using MALDI-TOF mass spectrometry as S1, another ribosomal protein. The identity of L13, L22, and L24 were also confirmed by MALDI-TOF mass spectrometry.

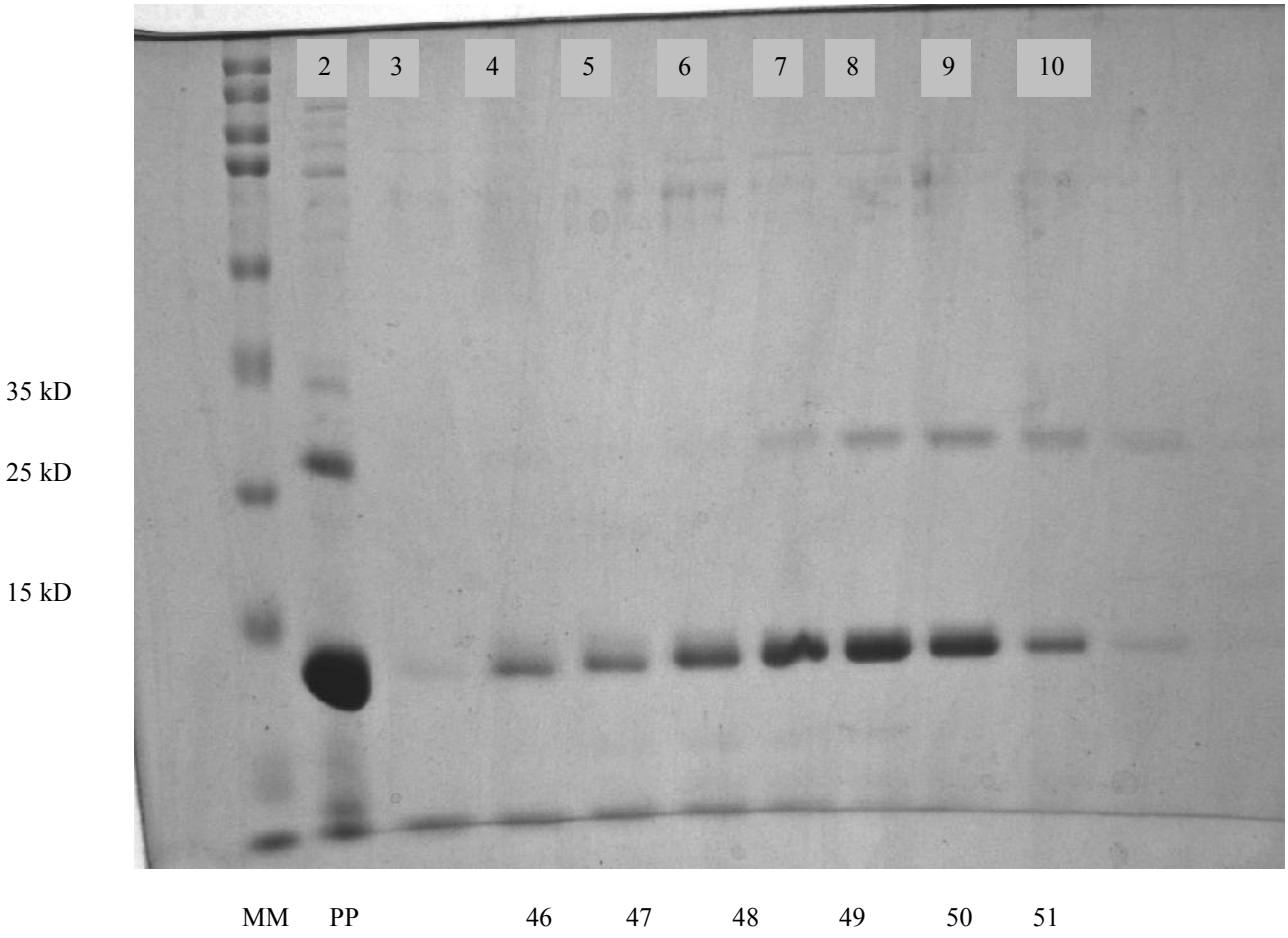

Figure 4.1 SDS-PAGE gel of L13 purification. Lane 1 molecular weight markers; lane 2 previously purified L13; and lanes 4-11 fractions from SP-Sepharose column (fractions 46-51).

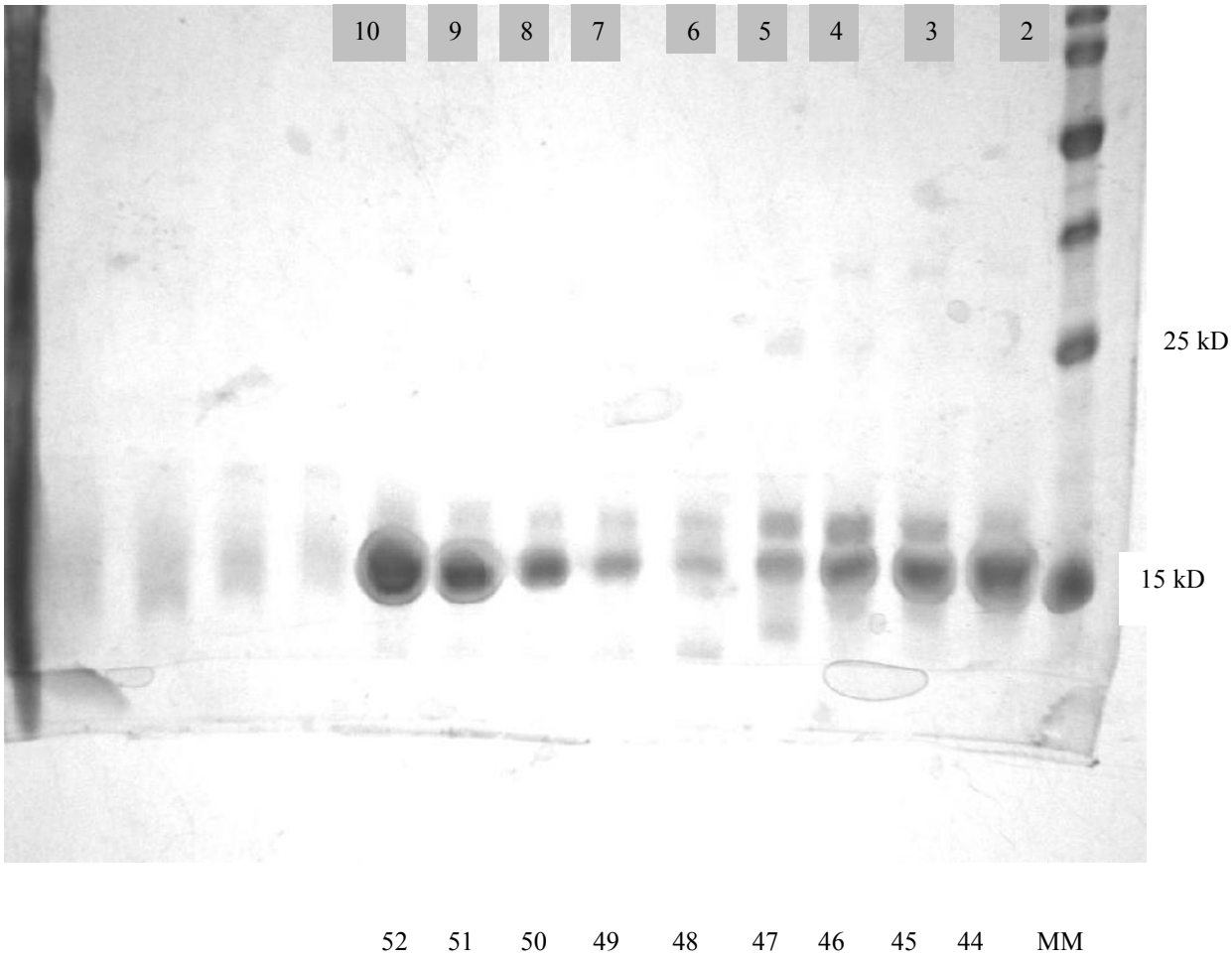

Figure 4.2 SDS-PAGE gel of L22 purification, from right to left. Lane 1 molecular weight markers; and lanes 2-10 fractions from SP-Sepharose column (fractions 44-52).

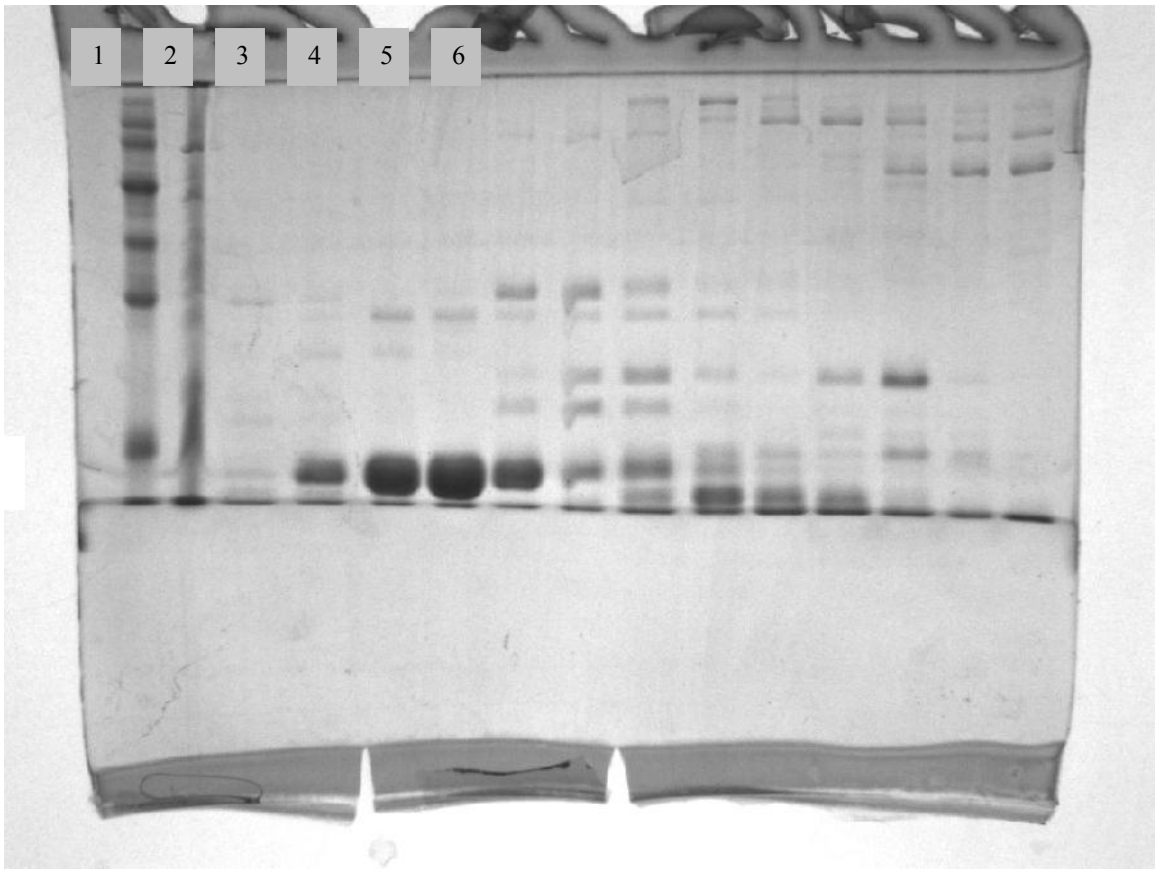

Figure 4.3 SDS-PAGE gel of L24 purification. Lane 1: molecular weight markers; lane 2 crude extract L24; and lanes 4-6: fractions from SP-Sepharose column (fractions 46, 48, and 50).

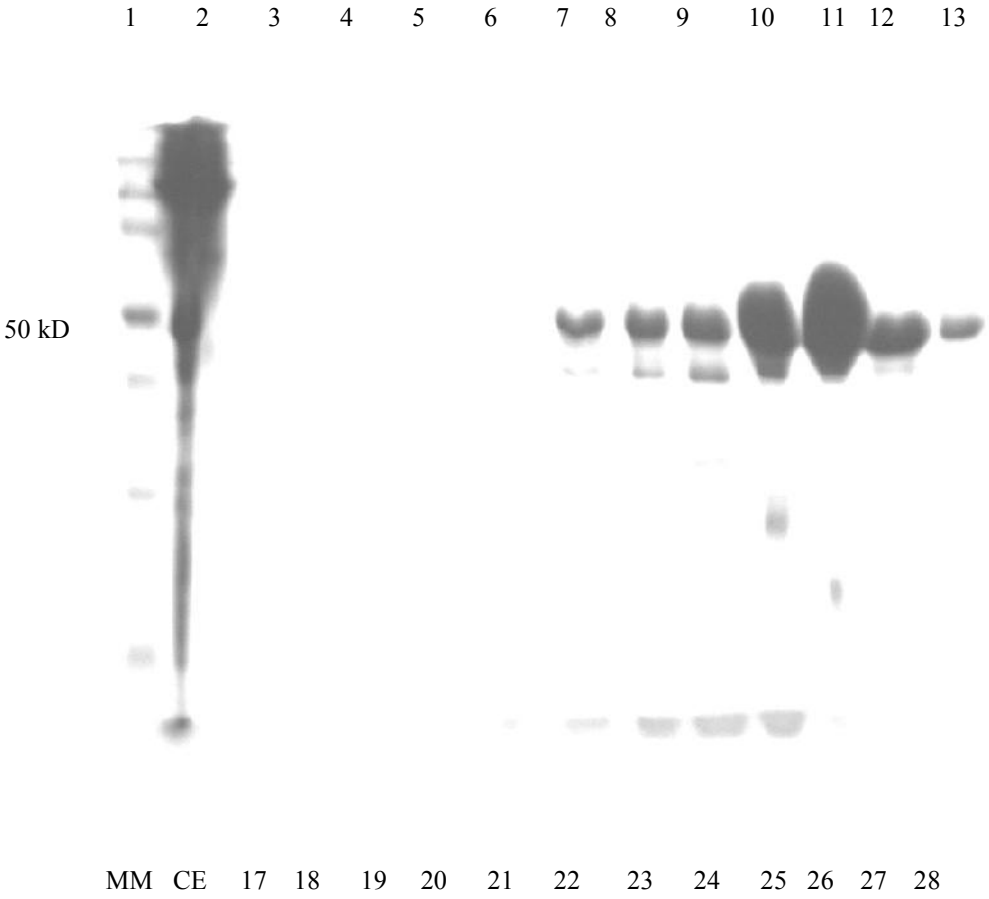

Figure 4.4 SDS-PAGE gel of MBP-L29 purification. Lane 1 molecular weight markers; lane 2 crude protein extract; and lanes 6-12 fractions from Amylose column (fractions 22-28).

Elemental analyses demonstrated that none of the proteins (L13, L22, L24, and L29) bound any significant amount of metal directly after purification. To further probe for metal binding all of the proteins were individually incubated with up to 10 equivalents of Zn(II) for thirty minutes on ice. The resultant proteins were individually dialyzed versus 2 changes of 2 L of 25 mM Tris-Cl, pH 8.5, for four hours per dialysis at 4 ^{o}C. L22, L24, and L29 were analyzed again after dialysis, no significant amounts of metal were detected. L13 did bind 0.6 equivalents of Zn(II).

Table 4.1. Metal Analyses of L13, L22, L24, and MBP-L29

Protein	**Zn(II) (equivalents)**
L13 as-purified	<0.01
L13 metal-loaded	0.6 ± 0.1
L22 as-purified	<0.01
L22 metal-loaded	<0.01
L24 as-purified	<0.01
L24 metal-loaded	<0.01
MBP-L29 as-purified	<0.01
MBP-L29 metal-loaded	<0.01

4.4 Discussion

One of the essential assumptions of the proposed co-translational model for bacterial Zn(II) homeostasis is the ability of ribosomal proteins to transfer Zn(II) to nascent proteins as they exit the polypeptide exit tunnel. The polypeptide exit site is encircled by several ribosomal proteins (Figure 4.5). These include the universally-conserved L22, L23, L24, and L29 proteins (4). L22 lines the peptide tunnel (4). L23 is the central anchoring point for the signal recognition particle (SRP) and trigger factor (4). L24 is present at the tunnel as is L29 (4). The ring of proteins around the tunnel form a halo shaped platform (Figure 4.5) (4). It is on this platform that the transfer of Zn(II) from the ribosome to nascent Zn(II) metalloproteins was hypothesized to occur. L23 was excluded as a possible ribosomal protein that participates in metallation given the fact that it is a docking site and thus would be blocked by SRP and trigger factor (4). L22, L24, and L29 were cloned, over-expressed, purified, and analyzed for Zn(II) binding to gather evidence for their possible participation in Zn(II) metallation. It is proposed that these proteins would bind Zn(II) with novel metal binding sites with small numbers of protein ligands, similar to those sites found for ZnuA (7) and L31 (Chapter 2). Elemental analyses showed that no Zn(II) was bound by L22, L24, and L29 while isolated in solution. It is possible that the lack of Zn(II) binding in L22, L24, and L29 maybe due to improper folding.

However, these proteins were produced in a soluble form and Zn(II) structural sites generally do not require any complex tertiary or quaternary structure for Zn(II) binding (8).

In an effort to expand the search for Zn(II) binding ribosomal proteins, L13, which was identified in the aforementioned proteomic studies (3), was cloned, over-expressed, and characterized for Zn(II) binding. L13 was shown to bind 0.6 equivalent of Zn(II). We believe that the non-stoichiometric amounts of Zn(II) is due to an error in calculation of protein concentration or to the possibility that the binding affinity to the Zn(II) site in L13 may be low. While the previously reported proteomic studies (3) are problematic due to a in-gel refolding procedure, these studies did predict that L13 was a potential Zn(II) metalloprotein. Our results confirm this prediction. The other potential Zn(II) bind ribosomal proteins (L2, S2, S15, S16, and S17) need to be expressed, purified, and analyzed for Zn(II) binding to unequivocally confirm these predictions. These results indicate that the proteins surrounding the polypeptide exit tunnel do not bind zinc. This result will require a modification to be made in the co-translational model of Zn(II) homeostasis to account for Zn(II) transfer to nascent proteins. This modification is proposed in the concluding chapter of this dissertation.

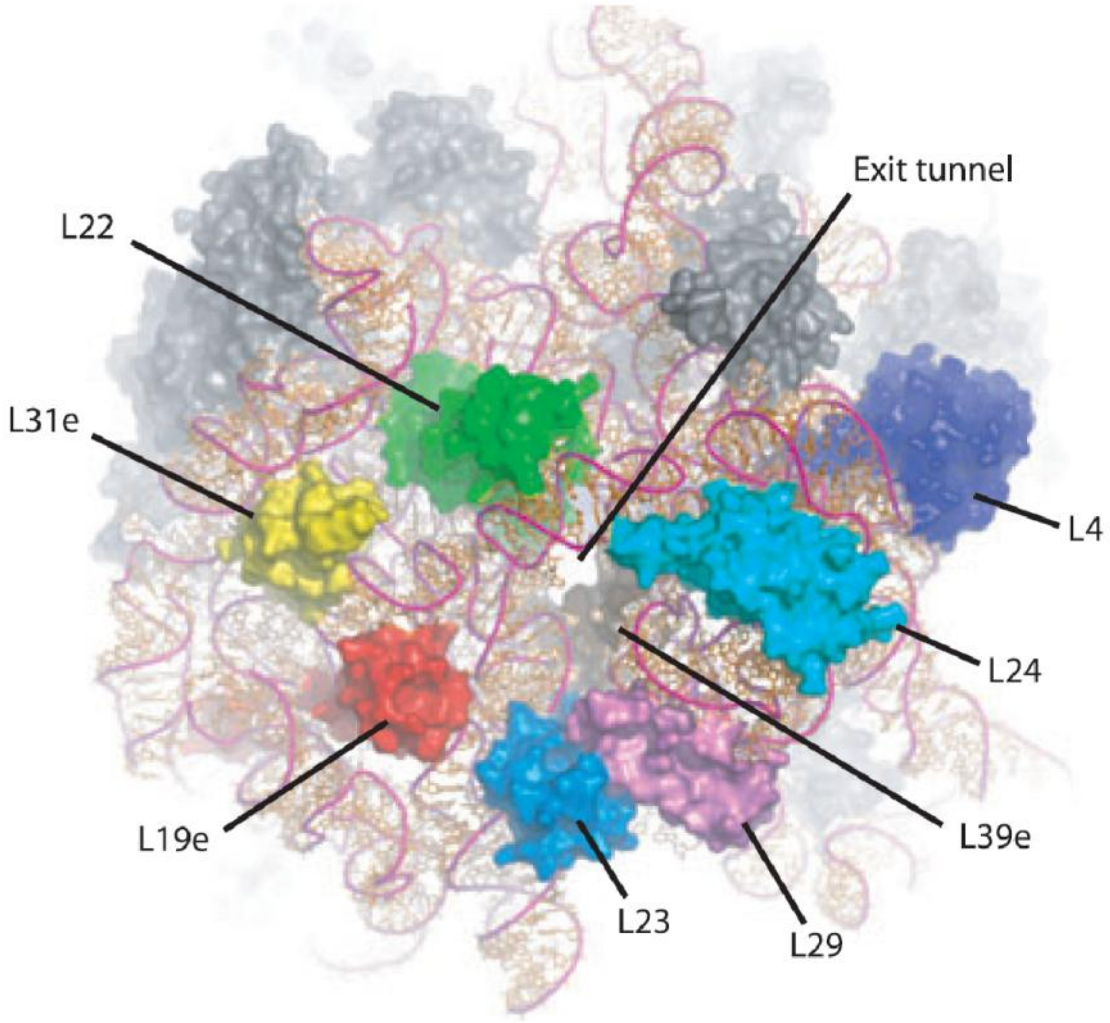

Figure 4.5 The exit of the polypeptide tunnel on the 50S subunit. The 50S subunit is viewed down the tunnel from the exit at the back of the 50S subunit. The 23S rRNA is shown in ribbon model while the ribosomal proteins are in a space filling model. This figure was taken from (4).

4.5 Acknowledgements

The author would like to thank Lauren Spadafora for her assistance in protein isolation and handling.

4.6 References

1. Nanamiya, H., Akanuma, G., Natori, Y., Murayama, R., Kosono, S., Kudo, T., Kobayashi, K., Ogasawara, N., Park, S., M., Ochi, K., and Kawamura. F. (2004) Zinc is a key factor in controlling alternation of two types of L31 protein in *Bacillus subtilis*. *Mol. Microbol*. 52(1), 273-283

2. Hard, T., Rak, A., Allard, P., Kloo, L., and Garber, M. (2000) The solution structure of ribosomal protein L36 from *Thermus thermophilus* reveals a zinc-ribbon-like fold. *J. Mol. Biol.* 296, 169-180.

3. Katayama, A., Tsujii, A., Wada, A., Nishino, T., Ishihama, A. (2002) Systematic search for zinc-binding proteins in *Escherichia coli*. *Eur. J. Biochem.* 269, 2403-2413.

4. Brodersen, D., E., and Nissen, P. (2005) The social life of ribosomal proteins. *FEBS J.* 272, 2098-2108.

5. Bradford, M., M. (1976) A rapid and sensitive method for the quantitation of microgram quantities of protein utilizing the principle of protein-dye binding. *Anal. Chem.* 72, 248-254.

6. McGafferty, D., Lessard I., & Walsh C. (1997) Mutational analysis of potential zinc-binding residues in the active site of the enterococcal *D*-Ala-*D*-Ala dipeptidase VanX. *Biochemistr*y. 36, 10498-10505.

7. Yatsunyk, L., A., Easton, J., A., Kim, L., R., Sugarbaker, S., A., Bennett, B., Breece, R., M., Vorontsov, I., I., Tierney, D., L., Crowder, M., W. (2008) Structure and metal binding properties of ZnuA, a perplasmic zinc transporter from *E. coli. J. Biol. Inorg. Chem.* 13(2), 271-288.

8. Cox, E., H., and McLendon, G., L., (2000) Zinc-dependent protein folding. *Curr. Opin. Chem. Biol.* 4, 162-165.

Chapter 5
Conclusions

5.1 Perspectives on metal ion homeostasis in prokaryotes

From the study of the complete genomes sequenced to date and the following primary sequences of the potential proteomes, it is estimated that one out of every three proteins requires a metal cofactor (1). Given the abundance and important structural and catalytic roles metals perform in biological systems, there must be mechanisms in place for the regulation of absorption, distribution, cellular uptake, and excretion of transition metals. These mechanisms must exist because many metal ions are essential for the viability of cells; however, these same metals are toxic if their intracellular concentrations become too high.

Metal ion homeostasis has been extensively studied in *E. coli* (2, 3, 4, 5), and like in eukaryotes, the intracellular levels of all metal ions must be maintained at optimal concentrations. Total Zn(II) concentrations in *E. coli* cells have been reported by O'Halloran and others to be *ca*. 2 x 10^5 atoms per cell (millimolar concentrations) (6). It was thought by many that there existed pools of "free" (*i.e*., readily available) Zn(II) in the cytoplasm of cells. By using a transcription factor-based assay, O'Halloran's group showed that the concentration of "free" Zn(II) in the cell at equilibrium is 10^{-15} M, which is about one free atom of Zn(II) per cell (6). O'Halloran attempted to identify all of the Zn(II) binding proteins and ascertain their copy numbers to account for the millimolar concentrations of Zn(II); however, only 12% of 0.2 mM cellular Zn(II) could be accounted for by O'Halloran (6).

Our model for Zn(II) homeostasis in *E. coli* proposes that a large portion of total cellular Zn(II) is being stored in the ribosome and that this Zn(II) is being delivered to Zn(II) metalloproteins as they are being translated. We hypothesize that this process of co-translational insertion of Zn(II) involves ribosomal proteins. This process would involve Zn(II) ions specifically being released from ribosomal proteins upon contact with their cognate Zn(II) metalloproteins and metal transfer to proceed through ligand substitution.

5.2 Approaches taken

In an effort to better understand Zn(II) trafficking, several groups have reported proteomic and cDNA microarray experiments to study the effects of Zn(II) excess and deficiency

(2, 3, 4, 5). The rationale for these studies is that the expression levels of genes/proteins involved in Zn(II) homeostasis would be affected by cytoplasmic Zn(II) levels. Despite the universality of the metallochaperone model for metal ion transport (7, 8, 9, 10), there have been no cytoplasmic Zn(II) metallochaperones yet identified in any organism. The fundamental assumption for previous proteomic and genomic studies of Zn(II) homeostasis is that a Zn(II) metallochaperone would be directly regulated by cytoplasmic Zn(II) levels. This assumption appears to be incorrect.

In the co-translational model for Zn(II) homeostasis, the first previously reported data that must be accounted for is the presence of the 0.2 mM Zn(II) in *E. coli* (6). This condition is met by demonstrating that the ribosome stores large amounts of cellular Zn(II) and that Zn(II) is bound by ribosomal proteins. This ribosomal storage is essential to the co-translational model, given the lack of sub-cellular compartmentalization in *E. coli*. There are potentially an infinite number of ligands (proteins, nucleic acids, small molecules) available to bind to Zn(II). However, a very delicate balance must exist so that Zn(II) is available to metallate Zn(II) metalloproteins but not too readily available to constantly metallate ZntR and Zur, the Zn(II) metallo-regulators (6). The first step in supporting this ribosomal storage hypothesis is to determine if Zn(II) actually binds to the *E. coli* ribosome. In Chapter 1 we showed that the ribosome binds significant amounts of Zn(II), and spectroscopic evidence strongly suggests that the ribosomes bind Zn(II) using proteins rather than nucleic acids. By using literature searches in light of our findings, we were able to offer a list of potential ribosomal proteins that could bind Zn(II) (11, 12, 13). Our studies show the as-isolated whole 70S ribosome binds eight equivalents of metal, which could be located in eight ribosomal proteins (L2, L13, L31, L36, S2, S15, S16, and S17). Our finding that the ribosome binds eight equivalents of Zn(II) allows us to account for a large percent, 0.02-0.52 μM ribosomal Zn(II) depending upon growth, of the predicted 0.2-0.8 μM cytoplasmic Zn(II) in *E. coli*.

In previous studies examining Zn(II) deficiency, one of the only consistent results is a large up-regulation of *ykgM* in response to low Zn(II) conditions (2, 4, 14). YkgM is a hypothetical ribosomal protein under the control of the Zn(II) metalloregulator Zur (4). While the function of YkgM in *E. coli* is unknown, a role has been proposed for a similar protein in *B. subtilis*. In *B. subtilis* ribosomal protein L31 and its homolog protein YtiA have recently been hypothesized to participate in a Zn(II) starvation model (15). Under Zn(II) limiting conditions,

the Zn(II) binding ribosomal protein L31 (called C+ because it contains two CXXC motifs that are thought to bind Zn(II)) is replaced with the non Zn(II)-binding paralog YtiA (called C- because of the lack of the CXXC motifs found in L31) (12). The replacement of Zn(II)-loaded L31 with YtiA, which does not bind Zn(II), is thought to mobilize ribosome-associated Zn(II), by releasing Zn(II)-loaded L31 into the cell (15). L31 is thought to be degraded, and a significant amount of Zn(II) is released into the cell, while ribosome function is maintained (15). This Zn(II) starvation model suggests that the ribosome may serve as a cellular reservoir of Zn(II).

In Chapter 3 we describe studies on *E. coli* L31. L31 was cloned, over-expressed, purified, and subjected to characterization in an attempt to gain evidence for a Zn(II) starvation mechanism. The data show that L31 binds 1.2 equivalents of Zn(II) and that YkgM binds no Zn(II) (Easton unpublished). Spectroscopic and mutagenesis studies on L31 demonstrate that the Zn(II) binding motif of L31 contains one cysteine, one histidine residue, and two to three non histidine N/O ligands. Nonetheless, an examination of the crystal structure of L31 when bound to the ribosome shows no Zn(II) binding (Figure 3.6 in Chapter 3) (16). In addition, it is not possible for all four cysteine residues in L31 to be bound to Zn(II) when L31 is bound to the ribosome. Our data show that L31, while isolated in solution, adopts a conformation that binds roughly one molar equivalent of Zn(II). While a Zn(II) starvation mechanism may exist in *E. coli* as it was articulated for *B. subtilis*, details of this mechanism remain unknown, and future studies are needed to demonstrate such a model in *E. coli* (15). In an effort to gather more evidence for a Zn(II) starvation mechanism in *E. coli* further investigations were conduced into previous crystal structures (17). A bona fide C+/C- paralogous pair was identified: YkgO/L36. YkgO has been shown to be regulated by Zur (18) and thus under the control of Zn(II). Future studies will focus on YkgO/L36 to determine if these ribosomal paralogs participate in a Zn(II) starvation mechanism in *E. coli* in conjunction with YkgM/L31.

In our initial co-translational model for Zn(II) homeostasis, one of the possible means of transfer of Zn(II) from the ribosome to the nascent Zn(II) metalloproteins is a direct transfer from ribosomal proteins localized around the exit tunnel of the ribosome. To test whether any Zn(II) is localized near the polypeptide exit site in the large subunit of the ribosome, the universally conserved ribosomal proteins L22, L24, and L29 were cloned, over-expressed, and characterized for Zn(II) binding (Chapter 4). These three proteins are immediately adjacent to

the polypeptide exit site. No Zn(II) was found in the as-isolated or Zn(II)-treated L22, L24, or L29 proteins. This result is consistent with the lack of any known Zn(II) binding motifs in these three proteins. In an effort to expand our search for Zn(II) binding ribosomal proteins, L13 was cloned, over-expressed, purified, and subjected to elemental analysis. L13 bound no Zn(II) as-isolated; however, L13 did bind 0.6 equivalents of Zn(II) when incubated (and subsequently dialyzed) with Zn(II) prior to analysis. While L13 is not adjacent to the polypeptide exit site, its ability to bind Zn(II) does confirm previous evidence suggesting that it may bind Zn(II) (11).

The results in this dissertation require a modification of our Zn(II) insertion/co-translational model because the proteins near the polypeptide exit tunnel do not bind Zn(II). Our discovery of a possible Zn(II) starvation system with the identification of one small Zn(II) binding protein, L31 in *E. coli* must also be incorporated into our modified model. It is possible that L31 could serve as Zn(II) metallochaperone within the cell.

In order for L31 to serve as a metallochaperone in the cell, it would need to be constitutively expressed. This continuous expression would mean it would be readily available to the cell under any condition. The expression of most ribosomal proteins is regulated post-transcriptionally (19). The rate of ribosomal protein synthesis is controlled by the activity of ongoing rRNA expression. In *E. coli* there are 19 ribosomal protein operons (18). The major mechanism for coordinating the rate of ribosomal protein synthesis is autogenous feedback regulation (19). This regulation works at the translational level. Generally one of the ribosomal proteins in the operon binds directly to its own mRNA (19). This binding occurs at the operator, which may be located either upstream of the first gene or between genes in the operon, and inhibits translation of the proteins encoded in the mRNA (19). The expression of L31 is not regulated by this feedback mechanism, though ten repressor proteins have been identified to date: those are S1, S4, S7, S8, S15, S20, L1, L4, L10, and L20 (19). These repressor proteins regulate S1, *alpha*, *str*, *spc*, S20, L11, S10, L10, and L35 operons, respectively (19). These data indicate that L31 may be constitutively expressed without any post-transcription regulation. It is possible that a constant amount of L31 is present in the cell at all times. This cellular pool of L31 is necessary for efficient ribosome synthesis by the cell. However, given the fact that only one copy of L31 is required per ribosome (19), it is likely that residual unbound L31 is left in the cytoplasm of the cell. We hypothesize that this unbound L31 is able to act as a Zn(II) metallochaperone.

Our results on L31 suggest that the protein adopts a conformation in solution in which the Zn(II) binds to Cys16 and possibly His30 (the closest His to Cys16 – 23 Å away) of L31 (16). Our UV-Vis data on L31 in solution demonstrate that the ligand field is very weak, and this could be due a non-idealized geometry (tetrahedral, square pyramid or trigonal bipyramid, or octahedral). This weak ligand field could produce a Zn(II) site that has a lower affinity for Zn(II) than does traditional Zn(II) structural sites. This weak Zn(II) binding site would make the Zn(II) much more labile in solution facilitating the transfer of Zn(II) from L31 to nascent Zn(II) metalloproteins through a ligand exchange mechanism.

Four ribosomal proteins (L31, L33, L36, and S14) are duplicated in several bacterial genomes (20). Previously L31 was the only duplication identified in *E. coli*; however, another duplication L36/YkgO has been discovered (18). When these ribosomal paralogs from various genomes were analyzed, a distinctive pattern of amino acid variation was discovered. Each protein comes in two types. The first version contains a pattern of two pairs of conserved cysteines (CXXC) (in *E. coli* L36 one cysteine is replaced by a histidine), and the second version does not contain these CXXC motifs (20). These duplications have been labeled C+/C- (20). Analysis indicates the C+ form is the ancestral state of these ribosomal proteins (20). From previous studies, some trends are evident. Thermophilic bacteria almost always have a C+ form of the proteins (20). These observations suggest that the C+ forms in bacterial thermophiles are adaptive: the C+ form may help to stabilize the ribosome at high temperatures (20). Given the fact that all C+/C- ribosomal proteins, with the exception of S14, are bacteria-specific may indicate a thermophilic stage in the early evolution of bacteria (20). The subsequent loss of some of these C+ forms of ribosomal proteins, as seen in *E. coli*, maybe due to the shift from a early thermophilic stage to non-thermophilic environment and the resulting lack of need for extra stability in the ribosome. If *E. coli* no longer needs the stabilizing force of the C+ forms of ribosomal proteins, why then was the C+ form of L31 retained? We argue that L31 has taken on another role in bacteria, that of a Zn(II) metallochaperone. It is because of this essential function that this C+ form was retained.

A genomic knockout mutant in *B. subtilis* of L31 displayed a slow growth phenotype in rich medium (21). A genomic knockout of YkgM in *E. coli* exhibited no phenotype when grown in rich medium; however, the same knockout under low Zn(II) conditions resembled a ZnuA knockout (disruption of ZnuABC Zn(II) importer), which displayed a slow grow phenotype for

the first 15 hours of growth (14). These results underscore the importance of L31 and YkgM to the cell.

The hypothesis that L31 is a Zn(II) metallochaperone, when combined with the previously proposed Zn(II) starvation model (15), can address these current data. In our co-translational model a pool of L31 exists continuously in the cell (Figure 5.1 A). Under Zn(II) replete conditions these proteins in solution loosely bind Zn(II), some of the L31 pool is used to assemble new ribosomes but some L31 would remain in solution. A large portion of the ribosomal protein pool would be in proximity to the ribosome due to the electrostatics of the very basic ribosomal protein and anionic character of the ribosome (Figure 5.1 A). The unbound Zn(II) loaded L31 would act as a Zn(II) metallochaperone by directly transferring Zn(II) to nascent Zn(II) metalloproteins through a ligand exchange mechanism (Figure 5.1 B) that is very similar to what has been proposed for the transfer of Cu(I) from ATX1 to Ccc2 (22). The apo L31 proteins remaining in the pool bind free Zn(II) as it enters the cell through direct interactions with the ZnuB and ZupT (Figure 5.1 A).

As the cell becomes Zn(II) deficient Zur activates the transcription of *ykgM* gene. This ribosomal paralog of L31 is incorporated into new synthesized ribosomes. The YkgM also displaces any existing L31 from ribosomes in the cell, releasing a large amount of L31 in the cell, presumably each L31 displaced from the ribosome would contain one Zn(II) ion. Though we were unable to find unequivocal evidence for Zn(II) bound L31 by investigating the current ribosome crystal structures available. This release of additional L31 in the cell would mobilize Zn(II) from the ribosome. YkgM may act as a indirect Zn(II) sensor that allows the cell to increase its ability to sequester Zn(II) by increasing the amount of unbound L31 present in the cell and mobilize some ribosome associated Zn(II) during low Zn(II) conditions. Under Zn(II) excess the pool of ribosomal protein chaperones would be saturated with Zn(II), and the excess free unbound Zn(II) would activate ZntR and the Zn(II) would be exported from the cytoplasm.

5.3 Future directions

L31 would not be the first ribosomal protein to have biological functions outside of their contribution to translation. S10 serves as an antiterminator of transcription of λ phage N protein in *E. coli* (21). As has been previously discussed, several ribosomal proteins regulate the expression of themselves and other ribosomal proteins through translational feedback (21).

Future experiments would focus on determining whether YkgM does replace L31 in *E. coli* under Zn(II)-deficient conditions. *E. coli* cells would be grown in normal medium and in Zn(II)-deficient medium. The ribosomes from each could be isolated, and western blots of the ribosomes using antibodies to L31 and YkgM could be used to prove whether or not YkgM replaces L31 on the ribosome during Zn(II) deficient conditions. Similar studies could be conducted on L36 and YkgO to evaluate whether they are a paralogous pair.

In vitro experiments testing L31 ability to transfer Zn(II) to Zn(II) metalloprotein L1 will test whether L31 is a metallochaperone or not. Zn(II)-loaded MBP-L31 would be incubated with a mature apo metallo-*beta*-lactamase L1 followed by size exclusion purification to separated the two proteins. Each purified protein would be tested by ICP to evaluate the metal content of each. If L1 was found to contain Zn(II) then steady state kinetics would be used to determined if the L1 is active. Parallel studies would be conducted using unfolded apo L1 and Zn(II) loaded MBP-L31 to evaluate where L31 can transfer Zn(II) to a unfolded protein.

A double knockout of L31/L36 of *E. coli* will be generated to test whether these proteins are essential. If the knockout strain is viable, this would indicate that there are other ribosome-associated proteins that are behaving as Zn(II)-metallochaperones or that all of the functions of these proteins can be assumed by the paralogs.

The study and understanding of Zn(II) transport and homeostasis in prokaryotes will serve as a model upon which further understand of metal ion transport can be built. It is hoped that the full understanding of the complete metabolism of Zn(II) will lead to deeper knowledge of other similar divalent metal ions species which do not participate in oxidation-reduction reactions in biological systems. Metal ions such as Mg(II) and Ca(II), who along with Zn(II) serve critical functions in biology. Our ribosome centered model can be applied to these other metals. This is because the mechanism of ribosomal protein metallochaperone mediated transport is a system that could accommodate other divalent metal ion species.

There is also the possibility that the co-translation insertion of Zn(II) into new synthesized polypeptides could serve as a nucleation point for protein folding of both Zn(II)-metallo and non-metallo proteins. The possibility that ribosomal protein Zn(II)-metallochaperones could be serving a dual role in protein folding is very exciting. In brief, this would require only a slight modification to our co-translational model of Zn(II) homeostasis. Zn(II) would serve as a means to recruit amino acid residues into a tentative secondary structure

in the local environment surrounding the Zn(II) ion. This local secondary structure would then serve to recruit additional secondary structure elements, thus nucleating the protein folding process. During this recruitment of additional secondary structure the initial Zn(II) site would most likely be disrupted leading to the loss of the Zn(II). This is an illustration of future directions that could be taken once Zn(II) homeostasis is fully articulated. The possibility of the ribosome actively participating in metal ion transport and homeostasis could have ramifications on many other important biological processes.

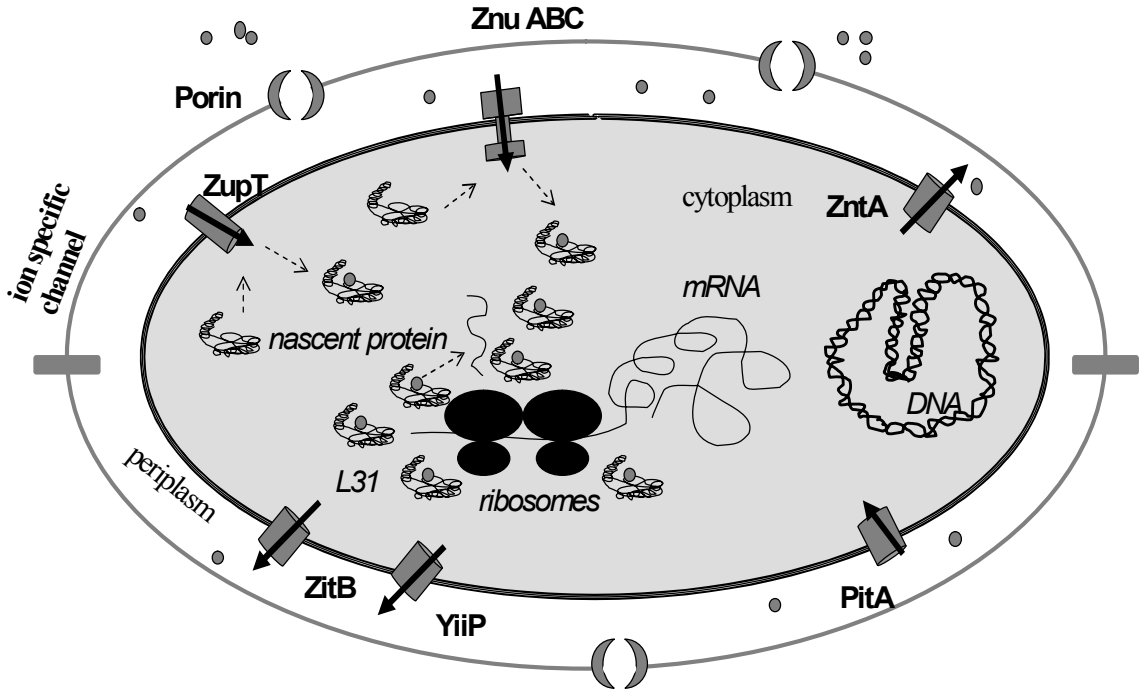
Znu ABC
Porin
ZupT
ion specific channel
cytoplasm
ZntA
mRNA
nascent protein
DNA
L31
ribosomes
periplasm
ZitB
YiiP
PitA

Figure 5.1 A

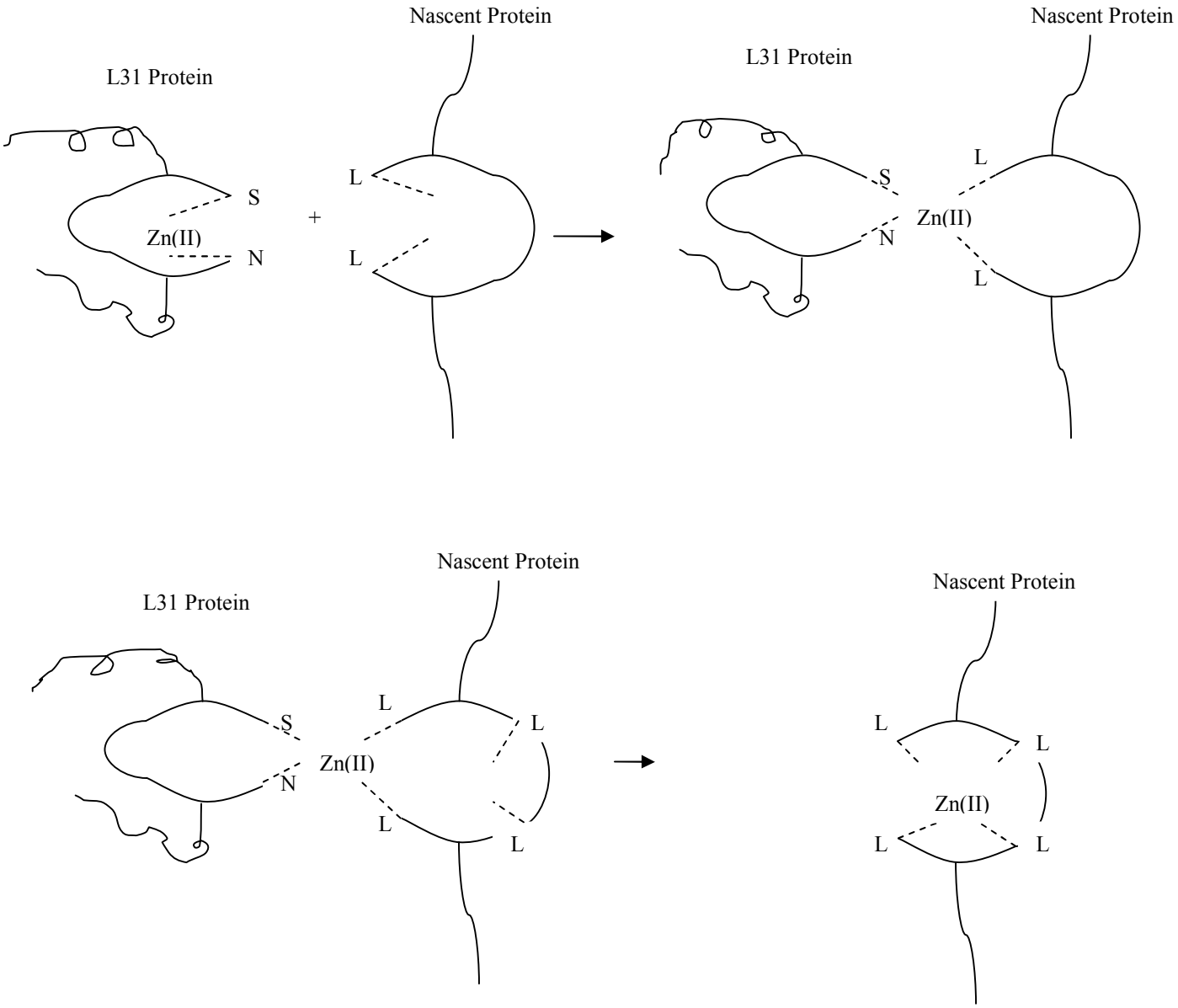
L31 Protein
Nascent Protein
S
Zn(II)
N
L
L
+
L31 Protein
Nascent Protein
S
N
Zn(II)
L
L
L31 Protein
Nascent Protein
S
N
Zn(II)
L
L
L
L
Nascent Protein
L
L
Zn(II)
L
L

Figure 5.1 B

Figure 5.1 Co-translational model of Zn(II) homeostasis. **A.** The unbound L31 binds one Zn(II) while in solution. The residual Zn(II)-loaded L31 loosely associate with the ribosome. This loosely associated L31 behaves as a metallochaperone while in solution transferring its Zn(II) to nascent proteins **B.** The method of insertion of Zn(II) involves a direct transfer from L31 to nascent protein through a ligand exchange mechanism. The formation of a temporary complex between L31 and nascent protein is under kinetic control. The temporary complex allows the nascent protein to recruit additional ligands which facilitates Zn(II) transfer. As the pool of unbound L31 becomes depleted of Zn(II) apo L31 will bind Zn(II) as it is imported into the cell from ZnuB and ZupT.

5.4 References

1. Mounicou, S., Szpunar, J., and Lobinski, R. (2008) Metallomics: The concept and methodology. *Chem. Soc. Rev.* 38, 1119-1138.

2. Brocklehurst, K. R., and A. P. Morby. (2000) Metal-ion tolerance in *Escherichia coli*: Analysis of transcriptional profiles by gene-array technology. *Microbiol.* 146, 2277-2282.

3. Lee, L. J., J. A. Barrett, and R. K. Poole. (2005) genome-wide transcriptional response of chemostat-cultured *Escherichia coli* to zinc. *J. Bacteriol*. 187, 1124-1134.

4. Sigdel, T. K., J. A. Easton, and M. W. Crowder. (2006) Transcriptinal response of *Escherichia coli* to TPEN. *J. Bacteriol*. 188, 6709-6713.

5. Yamamoto, K., and A. Ishihama. (2005) Transcriptional response of *Escherichia coli* to external zinc. *J. Bacteriol*. 187, 6333-6340.

6. Outten, C., E., and O'Halloran, T.,V. (2001) Femtomolar sensitivity of metalloregulatory proteins controlling zinc homeostasis. *Science* 292, 2488-2492.

7. Rosenzweig, T., V., and Culotta, V., C. (2002) Metallochaperones: bind and deliver. *Chem. Biol.* 9, 673-677.

8. O'Halloran, T., V., and Culotta, V., C. (2000) Metallochaperones, an intracellular shuttle service for metal ions. *J. Biol. Chem.* 275, 25057-25060.

9. Lin, Y., F., Walmsley, A., R., and Rosen, B., P. (2006) An arsenic metallochaperone for an arsenic detoxification pump. *Proc. Natl. Acad. Sci. U S A.* 103, 15617-15622.

10. Luk, E., Jensen, L., T., and Culotta, V., C. (2003) The many highways for intracellular trafficking of metals. *J. Biol. Inorg. Chem.* 8, 803-809.

11. Katayama, A., Tsujii, A., Wada, A., Nishino, T., Ishihama, A. (2002) Systematic search for zinc-binding proteins in *Escherichia coli*. *Eur. J. Biochem.* 269, 2403-2413.

12. Nanamiya, H., Akanuma, G., Natori, Y., Murayama, R., Kosono, S., Kudo, T., Kobayashi, K., Ogasawara, N., Park, S., M., Ochi, K., and Kawamura. F. (2004) Zinc is a key factor in controlling alternation of two types of L31 protein in *Bacillus subtilis*. *Mol. Microbol*. 52(1), 273-283.

13. Hard, T., Rak, A., Allard, P., Kloo, L., and Garber, M. (2000) The solution structure of ribosomal protein L36 from *Thermus thermophilus* reveals a zinc-ribbon-like fold. *J. Mol. Biol.* 296, 169-180.

14. Graham, A. I., Hunt, S., Stokes, S., L., Bramall, N., Bunch, J., Cox, A., G., McLead, C., W., and Poole, R., K. (2009) Severe zinc depletion of *Escherichia coli*: roles for high affinity zinc binding by ZinT, zinc transport and zinc-independent proteins. *J. Biol. Chem.* 284(27), 18377-18389.

15. Natori, Y., Nanamiya, H., Akanuma, G., Kosono, S., Kudo, T., Ochi, K., and Kawamura., F. (2007) A fail-safe system for the ribosome under Zn(II) limiting conditions in *Bacillus subtilis*. *Mol. Microbiol*. 63(1), 294-307.

16. Schuwirth, B., S., Borovinskaya, M., A., Hau, C., W., Zhang, W., Vila-Sanjurjo, A., Holton, J., M., Cate, J., H., D. (2005) Structures of the bacterial ribosome at 3.5 Å resolution *Science* 310, 827-834.

17. Dunkle, J., A., Xiong, L., Mankin, A., S., and Cate, J., H., D. (2010) Structure of the *Escherichia coli* ribosome with antibiotics bound near the peptidyl transferase center explain spectra of drug action. *P. Natl. Acad. Sci. U.S.A.* 107 (40), 17152-17157.

18. Hemm, M., R., Paul, B., J., Miranda-Rios, J., Zhang, A., Soltanzad, N., and Storz, G. (2010) Small stress proteins in *Escherichia coli*: Proteins missed by classic proteiomic studies. *J. Bacteriol.* 192(1), 46-58.

19. Kaczanowska, M., and Ryden-Aulin., M. (2007) Ribosome biogenesis and the translation process in *Escherichia coli*. *Microbiol. and Mol. Biol. Reviews*. 71(3), 477-494.

20. Makarova, K., S., Ponomarev, V., A., Koonin, E., V. (2001) Two C or nor two C: recurrent disruption of Zn-ribbons, gene duplication, lineage-specific gene loss, and horizontal gene transfer in evolution of bacterial ribosomal proteins. *Genome Biol.* 2(9), 33.1-33.14

21. Gabriel, S., E., and Helmann, J., D. (2009) Contributions of Zur-controlled ribosomal proteins to growth under zinc starvation conditions. *J. Bacteriol.* 191(19), 6116-6122.